The Astronomical Journal, 124:1001–1025, 2002 August
© 2002. The American Astronomical Society. All rights reserved. Printed in U.S.A.

NEAR-INFRARED PHOTOMETRIC VARIABILITY OF STARS TOWARD THE CHAMAELEON I MOLECULAR CLOUD

John M. Carpenter and Lynne A. Hillenbrand
Department of Astronomy, MS 105-24, California Institute of Technology, 1201 East California Boulevard, Pasadena, CA 91125;
jmc@astro.caltech.edu, lah@astro.caltech.edu

M. F. Skrutskie[1]
Department of Astronomy, University of Massachusetts, Amherst, MA 01003; mfs4n@virginia.edu

and

Michael R. Meyer
Steward Observatory, University of Arizona, 933 North Cherry Avenue, Tucson, AZ 85721; mmeyer@as.arizona.edu
Received 2002 March 28; accepted 2002 April 24

ABSTRACT

We present the results of a J, H, and K_s photometric monitoring campaign of a $0\overset{\circ}{.}72 \times 6^\circ$ area centered on the Chamaeleon I star-forming region. Data were obtained on 15 separate nights over a 4 month time interval using the Two Micron All Sky Survey south telescope. Out of a total of 34,539 sources brighter than the photometric completeness limits ($J = 16.0$, $H = 15.2$, and $K_s = 14.8$), 95 exhibit near-infrared variability in one or more bands. The variables can be grouped into a population of bright, red objects that are associated with the Chamaeleon I association and a population of faint, blue variables that are dispersed over the full 6° of the survey and are likely field stars or older pre–main-sequence stars unrelated to the present-day Chamaeleon I molecular cloud. Ten new candidate members of Chamaeleon I, including eight brown dwarf candidates, have been identified based on variability and/or near-infrared–excess emission in the $J-H$ versus $H-K_s$ color-color diagram. We also provide a compendium of astrometry and J, H, and K_s photometry for previously identified members and candidate members of Chamaeleon I.

Key words: infrared radiation — open clusters and associations: general — stars: pre–main-sequence — stars: variables: general

On-line material: additional figures

1. INTRODUCTION

Near-infrared variability provides a means to identify young stellar populations independent of most current observational selection techniques (e.g., Hα, Li, X-ray, and near-infrared–excess surveys) and has been shown to be sensitive to stars both with and without circumstellar accretion disks (Skrutskie et al. 1996). Variability studies, therefore, help provide a more complete census of the stellar population in star-forming regions. In the first (Carpenter, Hillenbrand, & Skrutskie 2001, hereafter CHS01) of a series of papers on the near-infrared photometric variability properties of pre–main-sequence objects, we analyzed J, H, and K_s time-series data of nearly 18,000 stars distributed over a $0\overset{\circ}{.}84 \times 6^\circ$ region toward the Orion A molecular cloud using observations conducted with southern Two Micron All Sky Survey (2MASS) telescope. The vast majority of the $\sim$1200 stars with time-variable JHK_s photometry identified in that study are young pre–main-sequence stars associated with the Orion molecular cloud. The large sample of variables was used to investigate the characteristics and origins of near-infrared variability in young stars.

A diversity of photometric behavior was observed during the $\sim$30 day time period encompassed by the Orion observations, including cyclic fluctuations, eclipses, aperiodic short-term fluctuations, slow drifts in brightness over the full length of the observing period, colorless variability, stars that become redder as they fade, and stars that become bluer as they fade. Rotational modulation by cool spots alone can explain the observed variability characteristics in $\sim$56%–77% of the stars, while the properties of the photometric fluctuations are more consistent with hot spots or extinction changes in at least 23% of the stars and with variations in the mass accretion rate or inner radius changes in the disk in $\sim$1% of the stars.

One limitation of the Orion survey is that at the distance of the Orion molecular cloud, the flux-limited observations were most sensitive to variability in stars more massive than 1 $M_\odot$. Observations of more proximate regions can use variability as a probe of lower mass stars and substellar objects and establish if the variability characteristics vary as a function of mass. Accordingly, we have conducted a near-infrared monitoring campaign of the Chamaeleon I star-forming region. At a distance of 160 pc (Whittet et al. 1997), Chamaeleon I is 3 times closer than the Orion molecular cloud and contains a moderately large sample of young pre–main-sequence stars ($\sim$120) that have already been identified (see Lawson, Feigelson, & Huenemoerder 1996 and references therein). Using the 2MASS south telescope, we observed a $0\overset{\circ}{.}72 \times 6^\circ$ region centered on the Chamaeleon I molecular cloud on 15 nights over a 4 month time period. These observations monitored over 34,000 stars with sensitivity to detect variability in young brown dwarfs with masses as low as $\sim$0.05 $M_\odot$.

The observations and data reduction procedures for this data set are described in § 2. In § 3, we identify the variable

[1] Current Address: Department of Astronomy, University of Virginia, P.O. Box 3818, Charlottesville, VA 22903.

stars from the time-series photometry, present light curves for all of the variable stars, and examine the spatial distribution and near-infrared photometric characteristics of the variable population. In § 4, we identify candidate members of Chamaeleon I based on near-infrared variability and also near-infrared excesses inferred from the time-averaged photometry. Our conclusions are summarized in § 5. A list of near-infrared photometry of known and candidate members of Chamaeleon I is provided in the Appendix.

2. DATA

2.1. *Observations and Data Processing*

The observing and data reduction procedures for the Chamaeleon I data closely follow that used in the Orion variability study. This section summarizes aspects of the data relevant specifically to the Chamaeleon I data. A more complete description of the data-processing procedures can be found in CHS01 and Cutri et al. (2000).[2]

The J, H, and K_s observations of Chamaeleon I were obtained with the 2MASS 1.3 m telescope at Cerro Tololo, Chile, near the completion of the southern survey operations when auxiliary projects were scheduled in otherwise idle telescope time. All data were collected in standard 2MASS observing mode by scanning the telescope in declination to cover tiles of size $(\Delta\alpha \times \Delta\delta) \sim (8\farcm5 \times 6^\circ)$ in the three bands simultaneously. The nominal region surveyed for this project consists of eight contiguous tiles in right ascension as listed in Table 1, with each tile centered on declination -77°. The total sky coverage is $\sim 0\fdg72 \times 6^\circ$. Observations were obtained on 15 separate nights, 13 of these in 2000 April and May and two in 2000 January when Chamaeleon I was observed as part of the normal 2MASS survey operations covering the entire sky (see Table 2). Complete coverage of all eight tiles was obtained on nine separate nights, while scheduling constraints limited observations to a subset of the eight tiles on the other six nights.

Adjacent tiles overlap by at least $40''$ in the 2MASS observing procedure to ensure complete coverage of the sky, as well as a check on the photometric repeatability of the observations. In practice, since the telescope is stepped slightly in right ascension while scanning a tile in declination, the amount of right ascension overlap changes with declination. For low-declination regions such as Chamaeleon I, there is near complete overlap at the southernmost declinations within a tile in order to maintain the minimum overlap in the north. Thus, for a large fraction of the sources, there is more than one measurement per night. Of the sources meeting the photometric completeness limits described in the following section, 53% have 12–14 photometric measurements, 38% of have 23–25 measurements, and the rest mainly have an intermediate number of measurements because of photometric incompleteness and nights with partial coverages.

The data were reduced using a development version of the 2MASS data-processing pipeline at the Infrared Processing and Analysis Center (IPAC) that also generated the data products for the 2MASS first and second incremental release catalogs. The data discussed in this paper, though, were not part of these incremental releases and will ultimately be replaced by the results of the final 2MASS processing. The 2MASS Explanatory Supplement (Cutri et al. 2000) contains complete details of the IPAC data reduction

[2] See http://www.ipac.caltech.edu/2mass/releases/second/doc/explsup.html.

TABLE 1
Coordinates of Observed Tiles

Tile	R.A.[a] (J2000.0)	Number of Nights Observed	
		Complete	Partial
1.....	11 04 38	18	3
2.....	11 06 15	22	3
3.....	11 07 46	26	3
4.....	11 09 23	28	3
5.....	11 10 55	26	3
6.....	11 12 31	21	3
7.....	11 14 02	16	3
8.....	11 15 39	16	3

Note.—Units of right ascension are hours, minutes, and seconds.

[a] Each tile is $8\farcm5 \times 6^\circ$ in size and is centered on a declination of -77° and the right ascension listed.

TABLE 2
Observing Log

UT Date	Tile 8	Tile 7	Tile 6	Tile 5	Tile 4	Tile 3	Tile 2	Tile 1	Comments
2000 Jan 13	X	X	X	X	X	X	X	X	$\delta < -78^\circ$ only
2000 Jan 25	X	X	X	X	X	X	X	X	$\delta > -78^\circ$ only
2000 Apr 8	X	...	X	X	X	X	X	X	...
2000 Apr 12.....	X	X	X	X	X	X	X	X	...
2000 Apr 19.....	...	...	...	...	X	X	X	X	...
2000 Apr 21.....	X	X	X	X	X	X	X	X	...
2000 Apr 22.....	X	X	X	X	X	X	X	X	...
2000 Apr 23.....	X	X	X	X	X	X	X	X	...
2000 Apr 24.....	X	X	X	X	X	X	X	X	...
2000 Apr 25.....	X	X	X	X	X	X	X	X	...
2000 Apr 27.....	X	X	X	...	X	...	...	...	...
2000 Apr 29.....	X	X	X	X	X	X	X	X	...
2000 May 1	X	X	X	X	X	X	X	X	...
2000 May 12.....	X	X	X	X	...	...	...	...	...
2000 May 19.....	X	X	X	X	X	X	X	X	...

procedures. As with the Orion data, the photometric zero point was adjusted by us for each tile using bright, isolated stars as secondary standards (see CHS01 for full description of the methods). On a few scans, the photometric offsets derived from the secondary standards deviated systematically from the mean offset by up to 0.1–0.2 mag over a $\Delta\delta \sim 0.^{\circ}5$ region of the 6° long tile. These photometric deviations are presumably caused by clouds passing overhead. For the affected region within a scan, the photometric offsets as a function of declination were computed by averaging the offsets for every 10–15 secondary standards. Photometric offsets were derived in this manner for portions of 13 scans out of a total of 108 scans observed for this project and affected only $\sim$1% of the total scan area.

2.2. *Point-Source List*

As a first step in generating the point-source list, we established the photometric completeness limit of the observations. Using data from the nine nights on which all eight tiles were observed (see Table 1), we empirically determined the magnitude limit at which a star is expected to be detected on at least eight of the nine nights in the absence of source confusion. The lack of a detection on the one night can be attributed typically to random noise that puts the star below the sensitivity limit of the observations. The completeness limit as defined here then is the magnitude at which there is a 89% chance that the star was detected on an appropriate apparition. This magnitude limit occurs at approximately $J = 16.0$, $H = 15.2$, and $K_s = 14.8$ for these data, corresponding to a signal-to-noise ratio of $\sim$7 as discussed below.

Our initial point-source list, generated from the nine nights in which all tiles were observed, contained 34,539 sources each having an average magnitude brighter than or equal to the photometric completeness limit in at least one band. Of these, $\sim$96% have no artifact or confusion flags from the processing pipeline in any of the observations. After removing those sources flagged as persistence or filter glints, potential lingering artifacts were identified as objects that had unusually blue colors for stars, were detected less than eight times, or had flags indicating contaminated or confused photometry from a nearby star. Many of these 1266 sources were visually inspected in the images, and sources deemed as artifacts were then removed from the point-source list. Criteria were established from this exercise to identify and remove likely artifacts for those sources not examined individually. Of the 34,539 stars meeting the magnitude completeness criteria, only 185 were deemed artifacts. The final source list for our variability analysis therefore contains 34,354 stars brighter than the defined completeness limits ($J = 16.0$, $H = 15.2$, and $K_s = 14.8$) in at least one band. Compared with the Orion observations (CHS01), Chamaeleon I contains nearly twice the number of sources (34,354 vs. 18,552), since it is both closer to the galactic center ($l = 297^{\circ}$ vs. 209°) and the galactic plane ($b = -16^{\circ}$ vs. -19°). However, the number of sources removed as artifacts is 4 times lower (185 vs. 744), since Chamaeleon I does not have the combination of high stellar density and bright nebulosity that makes photometry and source identification difficult in Orion.

To estimate the signal-to-noise ratio of the photometry, Figure 1 shows the observed photometric rms in the time series for each star as a function of magnitude. As discussed in CHS01, suspect photometric measurements for stars that are extended at the 2MASS resolution or have a high reduced χ^2 from a single point-spread function (PSF) measurement were excluded when computing the rms. Figure 1 shows a correlation with magnitude, as expected if the observed rms in the time series is due, primarily to photometric noise and not intrinsic variability. The observed rms values range from a minimum of $\sim$0.020 mag for the bright stars to $\lesssim$0.15 mag for stars near the completeness limit. The observed rms floor of $\sim$0.020 mag for the brighter stars is interpreted as the minimum photometric repeatability for these data, and consequently a minimum photometric uncertainty of 0.020 mag has been imposed on all of the photometric measurements. Based upon the estimated photometric uncertainties produced by the IPAC data reduction pipeline, we find that 99%, 90%, and 80% of the stars brighter than the respective completeness limits at J, H, and K_s have a signal-to-noise ratio per measurement $\geq$10, and 99% have a signal-to-noise ratio $\geq$7.

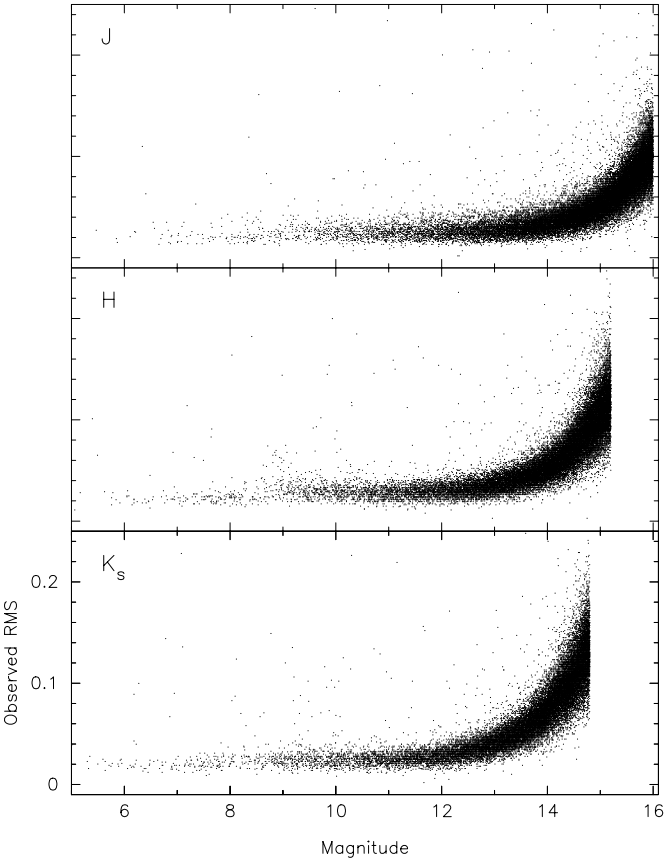

FIG. 1.—Observed photometric rms in the time-series data as a function of magnitude for stars brighter than the defined completeness limits. The observed rms ranges from $\sim$0.020 mag for the brightest stars to $\lesssim$0.15 mag (i.e., signal-to-noise ratio $\geq$7) for stars at the completeness limit. The scale on the y-axis is the same for each panel.

3. VARIABLE STARS IN THE CHAMAELEON I MOLECULAR CLOUD

3.1. *Identification*

Operationally, we define as a variable any star that exhibits larger photometric variations than expected over the course of a time series based upon the photometric uncer-

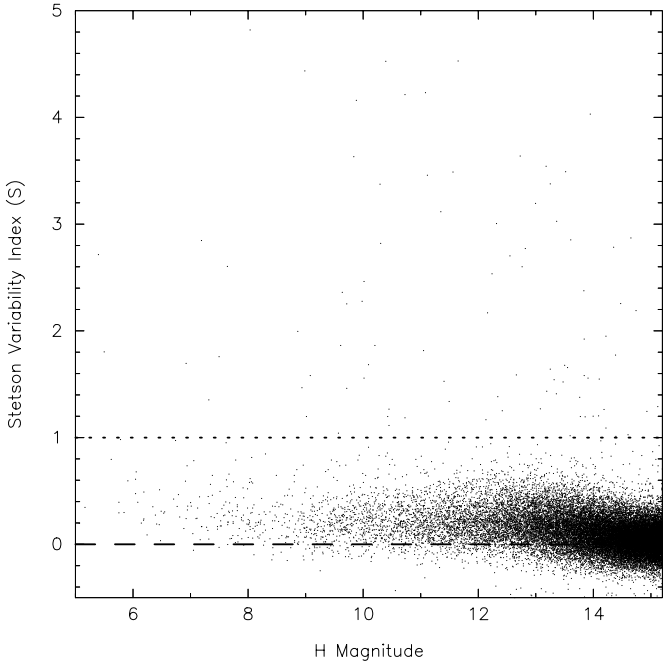

FIG. 2.—Stetson variable index (S) plotted as a function of the H magnitude for stars brighter than $H = 15.2$. The dashed line at $S = 0$ shows the expected value of the variability index for nonvariable stars. The origin of the positive bias in the computed index values is unknown and suggests that a weak correlation exists between the J, H, and K_s photometry, possibly from the fact that the three bands were observed at the same time. The dotted line at $S = 1.00$ represents the minimum adopted value used to identify variable stars in this study. Note that seven stars with $S > 5.0$ are not shown.

tainties. Following CHS01, we used the Stetson statistic (Stetson 1996), which correlates the photometric fluctuations observed in J, H, and K_s bands, as our primary means to identify candidate variable stars. As a secondary indicator, we also identified stars that have large reduced χ^2 in the time-series data but otherwise a small Stetson index. The light curves and images for each candidate variable star were visually examined; 17 stars were removed, and 12 stars that had a high reduced χ^2 but otherwise low Stetson index were added. The final list contains 95 variable stars.

Figure 2 shows the Stetson statistic (S) as a function of the H-band magnitude. For random noise, the Stetson variability index should be scattered around zero and have higher positive values for stars with correlated variability. As in the Orion analysis, the Stetson variability index for the Chamaeleon I objects has a positive value, on average, for brighter stars. The origin of this offset is unclear but is suggestive of a weak correlation between the J, H, and K_s photometry, possibly because of the fact that the three bands are observed simultaneously at each point in the time series. The minimum value of the Stetson variability index, which likely represents real photometric variability as opposed to random noise, was estimated by plotting the Stetson index versus the observed χ^2_ν and also from visual examination of the light curves as a function of the Stetson index. Variable stars were defined based on this analysis as objects having Stetson index $S \geq 1.00$. This threshold is larger than the value used for the Orion observations ($S = 0.55$), since the Orion data contained more photometric observations and consequently exhibited smaller scatter in the Stetson index.

Table 3 summarizes the photometric properties of the 95 variable stars identified from our data. Included in the table are an identification number, a common name for previously identified variable stars, the equatorial J2000.0 coordinates, the average J, H, and K_s magnitudes, the observed photometric rms, the number of high-quality photometric measurements used to assess the variability, and the Stetson variability index.

3.2. *Light Curves*

To illustrate the data obtained for this study, Figure 3 presents time-series photometry for the variable star 11344 (also known as T29 and Sz 22). This figure shows the J, H, and K light curves, the K_s vs. $H-K_s$ color-magnitude diagram, and the $J-H$ vs. $H-K_s$ color-color diagram. The electronic version of this article contains figures similar to Figure 3 for all 95 variable stars, but which also include the $J-H$ and $H-K_s$ light curves, the J vs. $J-H$ color-magnitude diagram, postage stamps of the J, H, and K_s images, and a tabular summary of the photometric data.[3]

As with the Orion observations, the variable stars in the Chamaeleon I data set show a diversity of behavior including gradual increases or decreases in the stellar brightness over the course of the time-series observations, decreases in the brightness on discrete days that may indicate an eclipsing system, colorless fluctuations, and instances where the colors become redder as the star fades. (Periodic variables were also identified in the Orion study, but a similar time-series analysis was not performed on the Chamaeleon I data because of the more limited, coarser time sampling.)

Most of the Chamaeleon I variables do not exhibit color variations with the brightness fluctuations. However, 14 of the variables exhibit observed dispersions in $J-H$ and $H-K_s$ colors more than 1.5 times larger than expected based on photometric noise. Figure 3 shows one example of color variability, which may be caused by either extinction variations or hot spots on the stellar surface (CHS01). After considering that up to half of the variable stars in Chamaeleon I may be field stars (see § 3.3 and 3.4), we conclude that ~15%–30% of the variables associated with Chamaeleon I show color variability. Similarly, 23% of the Orion variables show color variations of this type. No stars in Chamaeleon I become bluer as they dim, which is consistent with the results in Orion where only 1% of the variables exhibited these characteristics.

3.3. *Spatial Distribution of the Variable Stars*

The spatial distribution of variable stars identified in this study is presented in Figure 4. Also shown for comparison are (1) all sources in our point-source list with $J \leq 16.0$, (2) sources with a near-infrared excess detectable in the $J-H$ versus $H-K_s$ color-color diagram (see § 4.2), (3) 196 known or candidate members of the Chamaeleon I molecular cloud identified prior to this study (see Appendix), (4) X-ray sources selected from the *ROSAT* All-Sky Survey (Alcalá et al. 1995), and (5) an image of the average $H-K_s$ color in the

[3] Further, GIF images of these figures, links to tabular data, and cross references to existing optical and near-infrared catalogs are also currently available at the web site http://www.astro.caltech.edu/~jmc/variables/cham1.

TABLE 3

NEAR-INFRARED VARIABLE STARS

ID	NAME	COORDINATES (J2000.0)		MEAN MAGNITUDES			OBSERVED RMS			N			VARIABILITY INDEX
		α	δ	J	H	K_s	J	H	K_s	J	H	K_s	
198	...	165.860056	−78.387932	13.805	13.361	13.174	0.140	0.131	0.113	12	12	12	3.03
241	...	165.868449	−77.457493	13.889	13.254	12.988	0.094	0.080	0.076	13	13	13	1.64
670	...	165.915725	−76.944871	14.014	13.605	13.489	0.131	0.148	0.134	13	13	13	2.85
776	...	165.925563	−75.089402	13.678	13.078	12.898	0.053	0.053	0.060	13	13	13	1.27
1012	Hn 2	165.948566	−77.332334	11.353	10.449	10.044	0.044	0.051	0.048	13	13	13	1.27
1715	...	166.017772	−76.659153	12.906	11.651	10.837	0.203	0.161	0.129	13	13	13	4.53
1898	T14	166.037953	−76.455369	9.668	8.935	8.563	0.056	0.063	0.067	13	13	13	1.47
2168	...	166.062871	−76.110506	14.640	14.091	13.932	0.117	0.107	0.096	12	12	12	1.20
2225	...	166.068693	−76.469829	14.765	14.219	14.030	0.110	0.105	0.115	12	12	12	1.09
2745	...	166.122675	−76.938716	14.476	13.858	13.641	0.113	0.129	0.096	12	12	12	1.19
3131	...	166.161129	−74.019330	14.877	14.101	13.909	0.135	0.169	0.183	12	12	12	1.55
3616	...	166.207272	−75.686611	11.458	11.052	10.938	0.066	0.059	0.063	12	12	11	1.81
3841	...	166.234284	−74.561691	15.034	14.683	14.575	0.140	0.134	0.159	12	12	12	0.87
3876	T16	166.237490	−77.265824	12.245	10.974	10.498	0.448	0.296	0.359	16	16	17	7.83
4862	...	166.330871	−76.140610	14.069	13.597	13.470	0.101	0.097	0.096	24	24	24	0.78
6771	...	166.520456	−78.550732	11.862	11.495	11.380	0.061	0.057	0.066	13	13	13	1.34
8073	...	166.657725	−79.169620	12.924	12.417	12.273	0.071	0.098	0.079	24	24	24	1.25
8234	Hn 5	166.674016	−76.596987	11.588	10.727	10.177	0.072	0.059	0.039	24	24	24	1.19
8369	CHXR 20	166.687729	−77.450689	10.717	9.628	9.134	0.617	0.458	0.334	24	24	24	12.42
8978	T23	166.745878	−77.314854	11.195	10.429	9.999	0.044	0.051	0.049	24	23	23	1.20
9226	...	166.771953	−74.935493	13.841	13.521	13.421	0.146	0.162	0.147	24	24	24	3.49
9464	...	166.796780	−76.329690	13.696	13.180	13.037	0.192	0.185	0.172	24	24	24	3.54
9484	...	166.799142	−76.430582	13.667	12.904	12.466	0.066	0.054	0.041	24	24	24	0.62
9496	T24	166.800185	−76.539810	10.829	9.837	9.325	0.170	0.145	0.088	24	24	22	3.63
9652	ISO 97	166.817455	−77.385247	...	13.841	11.451	...	0.134	0.102	0	24	24	1.58
9847	T26	166.836317	−77.635363	7.810	6.941	6.224	0.021	0.034	0.040	23	23	23	0.74
10193	...	166.874272	−77.417151	12.163	11.353	10.958	0.121	0.112	0.111	17	19	16	3.12
10722	...	166.930706	−74.617254	13.937	13.525	13.412	0.072	0.041	0.056	12	12	12	0.33
10737	T28	166.931849	−77.661457	10.196	9.013	8.304	0.043	0.049	0.058	11	11	10	1.20
10937	...	166.950921	−75.989196	13.953	13.480	13.398	0.070	0.054	0.048	12	12	12	0.59
11188	...	166.975914	−73.965912	15.444	14.670	14.559	0.149	0.167	0.165	12	12	12	0.48
11315	CHXR 30b	166.988649	−77.290661	13.278	11.119	9.825	0.204	0.150	0.096	12	12	11	3.46
11344	T29	166.991301	−77.645848	10.147	8.406	7.107	0.262	0.182	0.136	11	11	11	5.49
11351	T30	166.991957	−77.711505	12.017	10.723	9.917	0.200	0.146	0.103	11	11	11	4.21
11462	T31	167.006145	−77.708036	8.692	7.640	6.947	0.083	0.083	0.090	18	15	17	2.60
11529	ISO 126	167.012202	−77.645213	11.574	9.636	8.205	0.095	0.093	0.070	16	18	20	2.36
11547	T32	167.013579	−77.654898	7.351	6.926	6.273	0.053	0.068	0.100	21	20	21	1.69
12029	...	167.061355	−79.484326	13.545	13.191	13.125	0.064	0.061	0.079	24	24	24	1.43
12055	T33	167.063875	−77.564862	8.356	7.189	6.182	0.119	0.114	0.089	19	25	25	2.85
12608	...	167.118568	−74.652561	14.263	13.777	13.643	0.064	0.078	0.103	25	25	25	1.20
12865	...	167.140347	−74.042462	13.034	12.547	12.426	0.083	0.086	0.089	25	25	25	2.70
13058	T35	167.162555	−77.267845	11.265	9.931	9.045	0.320	0.200	0.120	25	25	24	6.31
13577	...	167.213993	−77.277374	13.478	12.760	12.479	0.102	0.090	0.099	25	25	25	2.60
13616	T36	167.218164	−76.733232	13.535	12.993	12.809	0.165	0.123	0.113	24	25	24	3.19
13620	RX J1108.8−7519b	167.218439	−75.317429	10.521	9.711	9.365	0.085	0.051	0.045	15	16	15	1.46
13677	PU Car	167.223694	−75.360005	10.943	10.015	9.487	0.097	0.089	0.082	14	15	15	2.46
13707	T38	167.227553	−77.036964	11.448	10.304	9.549	0.162	0.114	0.067	24	25	24	2.82
13720	ISO 165	167.229063	−76.544769	13.137	12.164	11.523	0.100	0.083	0.051	23	24	21	2.17
14235	ISO 177	167.282989	−76.819620	12.771	11.945	11.658	0.187	0.154	0.156	13	13	13	5.38
14623	CHXR 79	167.325619	−76.508128	11.785	10.204	9.199	0.082	0.060	0.083	13	13	13	1.86
14800	C 1-6	167.344441	−76.575584	12.737	10.392	8.769	0.259	0.185	0.149	13	13	13	4.53
14843	T40	167.349170	−76.389109	10.064	8.986	8.121	0.164	0.144	0.124	13	12	13	4.43
15044	ISO 192	167.368966	−76.557816	16.108	13.320	11.044	0.140	0.126	0.105	13	13	13	1.54
15415	...	167.407585	−74.494542	13.069	12.657	12.533	0.055	0.074	0.061	13	13	13	1.59
15576	C 1-25	167.424641	−76.582928	13.764	11.405	10.075	0.082	0.058	0.067	21	19	21	1.52
15771	...	167.445696	−78.339541	12.647	12.237	12.103	0.098	0.098	0.102	24	24	24	2.53
15784	B43	167.447392	−77.441459	12.592	11.085	10.136	0.205	0.159	0.125	25	24	24	4.23
15991	...	167.468918	−77.676413	15.672	14.386	13.532	0.195	0.173	0.186	25	25	25	1.77
16026	T42	167.472503	−76.573776	9.612	8.032	6.782	0.246	0.164	0.144	25	25	25	4.82
16052	T43	167.475246	−76.490380	11.280	10.019	9.311	0.093	0.068	0.049	25	25	25	1.56
16067	ISO 225	167.476587	−76.519830	15.064	13.763	12.971	0.109	0.086	0.130	25	25	25	1.38
16096	C 1-2	167.479373	−76.544746	14.121	11.563	9.787	0.225	0.172	0.116	22	25	25	3.49
16254	T45	167.494498	−77.619185	9.948	8.863	8.099	0.078	0.065	0.087	25	25	25	2.00

TABLE 3—*Continued*

ID	Name	Coordinates (J2000.0)		Mean Magnitudes			Observed rms			N			Variability Index
		α	δ	J	H	K_s	J	H	K_s	J	H	K_s	
16307	T44	167.500391	−76.582762	8.777	7.319	6.180	0.073	0.063	0.043	25	25	25	1.35
16442	...	167.515876	−75.894432	12.529	12.320	12.231	0.109	0.116	0.118	25	25	25	3.01
16470	T45a	167.519496	−76.595892	10.530	9.609	9.221	0.069	0.069	0.060	25	25	25	1.86
17205	...	167.595185	−74.218745	14.615	13.946	13.774	0.251	0.214	0.257	12	17	12	4.03
18261	T47	167.706551	−77.297735	11.398	10.094	9.311	0.095	0.071	0.070	12	12	12	1.68
18403	T48	167.722205	−76.575567	11.214	10.445	9.956	0.046	0.037	0.051	12	12	12	1.11
18416	ISO 256	167.723233	−77.416833	13.999	12.242	11.156	0.398	0.312	0.219	12	11	12	8.11
18903	...	167.770410	−74.765601	15.042	14.389	14.206	0.110	0.141	0.115	12	12	12	0.94
18981	...	167.777547	−79.293338	14.230	13.502	13.289	0.092	0.089	0.100	25	25	25	1.68
19580	...	167.836748	−79.286170	13.546	13.355	13.262	0.077	0.061	0.070	25	25	25	1.41
20217	CHXR 48	167.894737	−76.605928	10.757	9.982	9.720	0.072	0.081	0.071	25	24	25	2.27
20409	T49	167.915282	−76.337519	10.552	9.718	9.180	0.072	0.102	0.135	25	25	25	2.25
21473	ISO 282	168.014564	−77.433591	13.286	12.323	11.682	0.314	0.226	0.152	25	25	22	6.73
21658	...	168.032510	−75.704201	12.990	12.732	12.674	0.135	0.134	0.138	13	13	13	3.64
21687	XZ Cha	168.035605	−78.911010	6.405	5.496	5.010	0.063	0.065	0.039	22	22	22	1.80
21745	T50	168.041012	−76.576841	11.108	10.296	9.870	0.113	0.117	0.073	13	13	13	3.37
22193	...	168.086269	−77.207763	14.549	13.838	13.567	0.129	0.086	0.131	13	13	13	1.92
22321	...	168.098276	−74.292164	13.685	13.249	13.141	0.145	0.154	0.144	13	13	13	3.38
22521	T52	168.115452	−76.739550	8.326	7.497	6.865	0.044	0.060	0.067	13	13	13	1.76
22662	T53	168.128869	−76.740037	10.975	9.878	9.209	0.234	0.154	0.106	13	13	13	4.16
22699	...	168.132021	−75.106479	14.523	14.222	14.152	0.171	0.130	0.136	13	13	13	1.95
23372	...	168.196514	−74.035743	14.317	13.907	13.834	0.098	0.112	0.119	13	13	13	1.56
25420	T55	168.389819	−76.593759	11.638	11.012	10.727	0.044	0.054	0.048	25	25	25	0.83
26688	...	168.505599	−78.862428	13.249	12.819	12.684	0.143	0.096	0.107	12	12	12	2.77
26728	YY Cha	168.509821	−76.909537	6.338	5.395	4.891	0.110	0.101	0.060	12	10	10	2.72
26963	...	168.532497	−76.602589	14.163	13.611	13.457	0.103	0.085	0.095	12	12	12	0.53
28089	...	168.636947	−76.712773	15.432	14.840	14.690	0.143	0.144	0.160	25	25	25	0.83
29102	...	168.730184	−77.759616	12.813	12.134	11.945	0.054	0.060	0.058	25	24	25	1.17
29730	...	168.783302	−79.022424	9.975	9.078	8.640	0.078	0.068	0.071	24	24	24	1.58
32775	...	169.066868	−74.273598	14.983	14.348	14.208	0.209	0.189	0.216	14	14	14	2.78
32930	...	169.080062	−74.427344	14.921	14.477	14.376	0.198	0.205	0.194	14	14	14	2.26
33139	...	169.097543	−74.461542	13.910	13.553	13.495	0.089	0.095	0.091	14	14	14	1.66

point-source list binned to a resolution of 5′. The overall density of stars increases from the south to the north, which reflects the decreasing distance (galactic latitude from −18° to −13°) to the galactic plane. Obscuration from dust in the Chamaeleon I molecular cloud is clearly manifested in a sharp decrease in the J-band star counts near the center of the image and a corresponding increase in the average $H-K_s$ color.

Variable stars are found over the entire 6° long region with a clear enhancement toward two regions in the molecular cloud at declinations of roughly −76.°5 and roughly −77.°5. The declination band between −76.°2 and −77.°8 that encompasses these two regions contains 63% (60/95) of the total number of identified variable stars despite containing only 27% of the survey area. The fact that the variable star surface density is highest toward the molecular cloud where the overall stellar density is lowest suggests direct affiliation of the variable stars with the molecular cloud and hence a young stellar population. Indeed, 45 of the 95 variable stars have been previously identified as likely members of the Chamaeleon I T Tauri association. Of the remaining 50 objects, 15 are projected against the molecular cloud and are discussed as possible Chamaeleon I members in § 4, and 35 are distributed over a larger region outside the molecular cloud boundaries. This widespread variable population may represent either variable field stars, intermediate-age (greater than 10 Myr) pre–main-sequence stars that have formed in the vicinity of the Chamaeleon I molecular cloud, or young (less than 10 Myr) pre–main-sequence stars formed in Chamaeleon I that have drifted from the molecular cloud. The data obtained here do not enable us to make a definitive interpretation of these variable stars, although, as discussed in the following section, the colors and magnitudes of these stars suggest they are not likely to be a young stellar population related to the Chamaeleon I molecular cloud.

3.4. *Colors and Magnitudes of the Variable Stars*

The nature of the variable stars can be clarified by analyzing their colors and magnitudes. At the sensitivity of the 2MASS observations, the field star population is dominated by main-sequence stars of spectral type late F to early K (see, e.g., Wainscoat et al. 1992). In contrast, most of the known members of Chamaeleon I have K and M spectral types (Lawson et al. 1996) and should have redder intrinsic colors than the field stars. Moreover, given the proximity and youth of the Chamaeleon I association, pre–main-sequence stars in Chamaeleon I will have brighter apparent magnitudes than the typical field star of the same spectral type.

To examine the colors and magnitudes for the stars detected in our observations, Figure 5 shows the K_s versus $H-K_s$ diagram for the variable star population (*circles*)

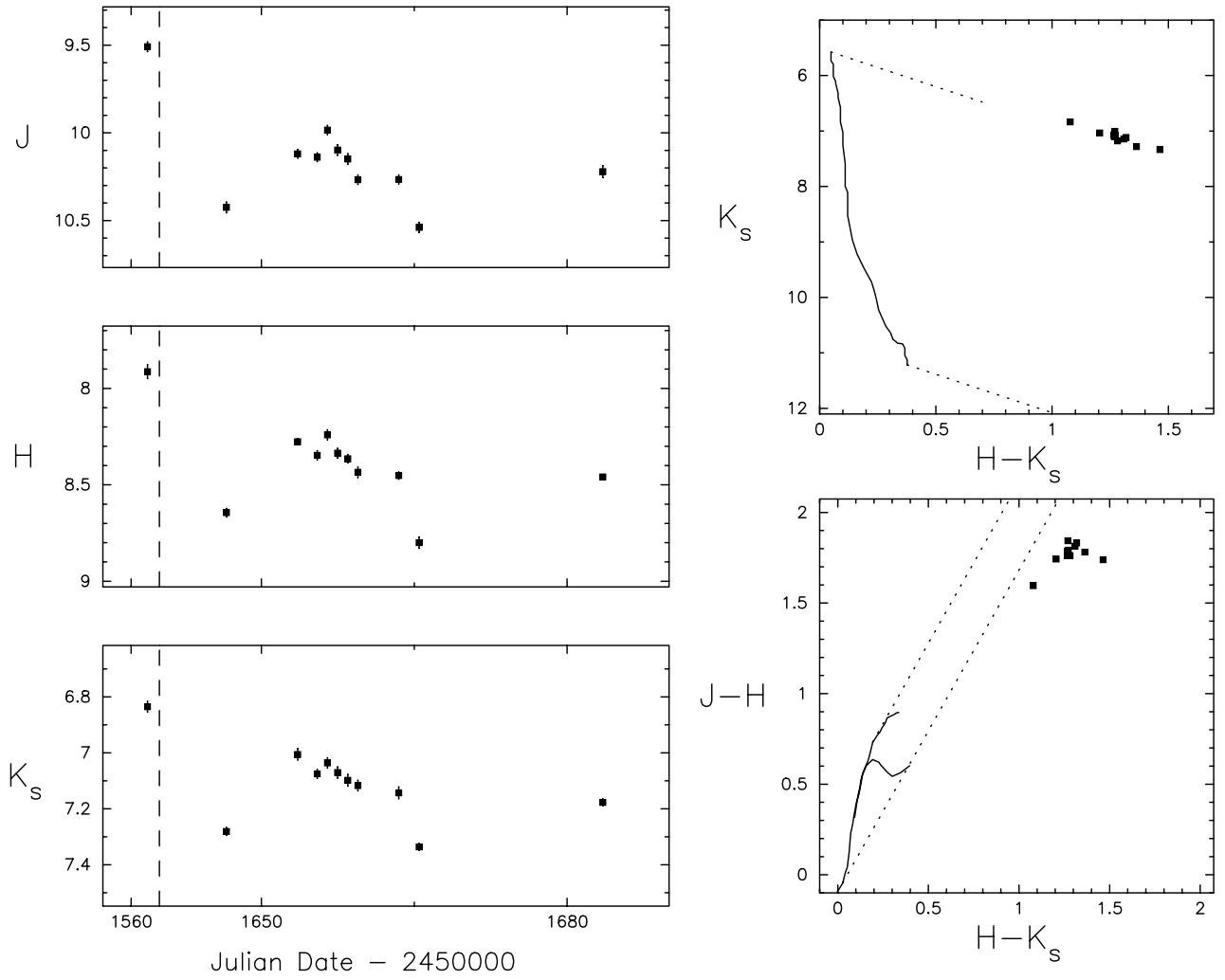

FIG. 3.—Photometric data for star 11344 (also known as T29 and Sz 22) that illustrates the data obtained for this study. The left panels show the J, H, and K_s, light curves. The vertical bars through the data points represent the $\pm 1\ \sigma$ photometric uncertainties. The right panels show the K_s vs. $H-K_s$ color-magnitude diagram and the $J-H$ vs. $H-K_s$ color-color diagram for each data point in the time series, where the dotted line represents the interstellar reddening vector from Cohen et al. (1981) transformed into the 2MASS photometric system (Carpenter 2001). The uncertainties in the stellar colors have been omitted for clarity. The solid line in the color-magnitude diagram is the 2 Myr pre–main-sequence isochrone from D'Antona & Mazzitelli (1997, 1998) for stellar masses between 0.08 and 3 $M_\odot$. The solid curves in the color-color diagram are the loci of red giant and main-sequence stars from Bessell & Brett (1988) in the 2MASS color system.

compared with all sources detected in the survey (represented in Hess format by the color scale). The filled circles indicate the subset of variable stars that have been previously identified as members or candidate members of Chamaeleon I (see Appendix). The black solid line in Figure 5 shows the 2 Myr pre–main-sequence isochrone from D'Antona & Mazzitelli (1997, 1998), corresponding to the mean age of the cluster (Lawson et al. 1996), and the dashed line shows the interstellar reddening vector. The variables can be coarsely grouped into two populations: (1) bright ($K_s \lesssim 12$) and red ($H-K_s \gtrsim 0.3$) stars and (2) relatively faint and blue stars. Most of the bright red variables are known members of Chamaeleon I with colors and magnitudes consistent with a young, reddened, pre–main-sequence population. Further, as shown in Figure 6, many of these red variables exhibit a near-infrared excess in the $J-H$ versus $H-K_s$ color-color diagram consistent with the presence of an optically thick circumstellar accretion disk (Lada & Adams 1992; Meyer, Calvet, & Hillenbrand 1997).

To further investigate the distinction between "red" and "blue" variable stars, Figure 7 shows the spatial distribution of variables separated by $H-K_s$ color, where the filled symbols again represent previously known Chamaeleon I members. Not surprisingly most of the red variable stars are found toward the Chamaeleon I molecular cloud and suggest that the red colors can be attributed to a combination of extinction, near-infrared–excess emission, and late spectral types for many of the association members. Four stars with red colors are found outside the boundaries of the Chamaeleon I molecular cloud. One of these variable stars is XZ Cha, thought to be a Mira star. A second is a suggested optical counterpart to a *ROSAT* X-ray source RX J1108.8−75919b and is likely a pre–main-sequence star (Alcalá et al. 1995). A third red variable is PU Car,[4] a vari-

[4] Alcalá et al. (1995) identified PU Car as RX J1108.8−7519b. However, based on the finding charts from Hoffmeister (1963), PU Car is located 2′.5 south of this X-ray source.

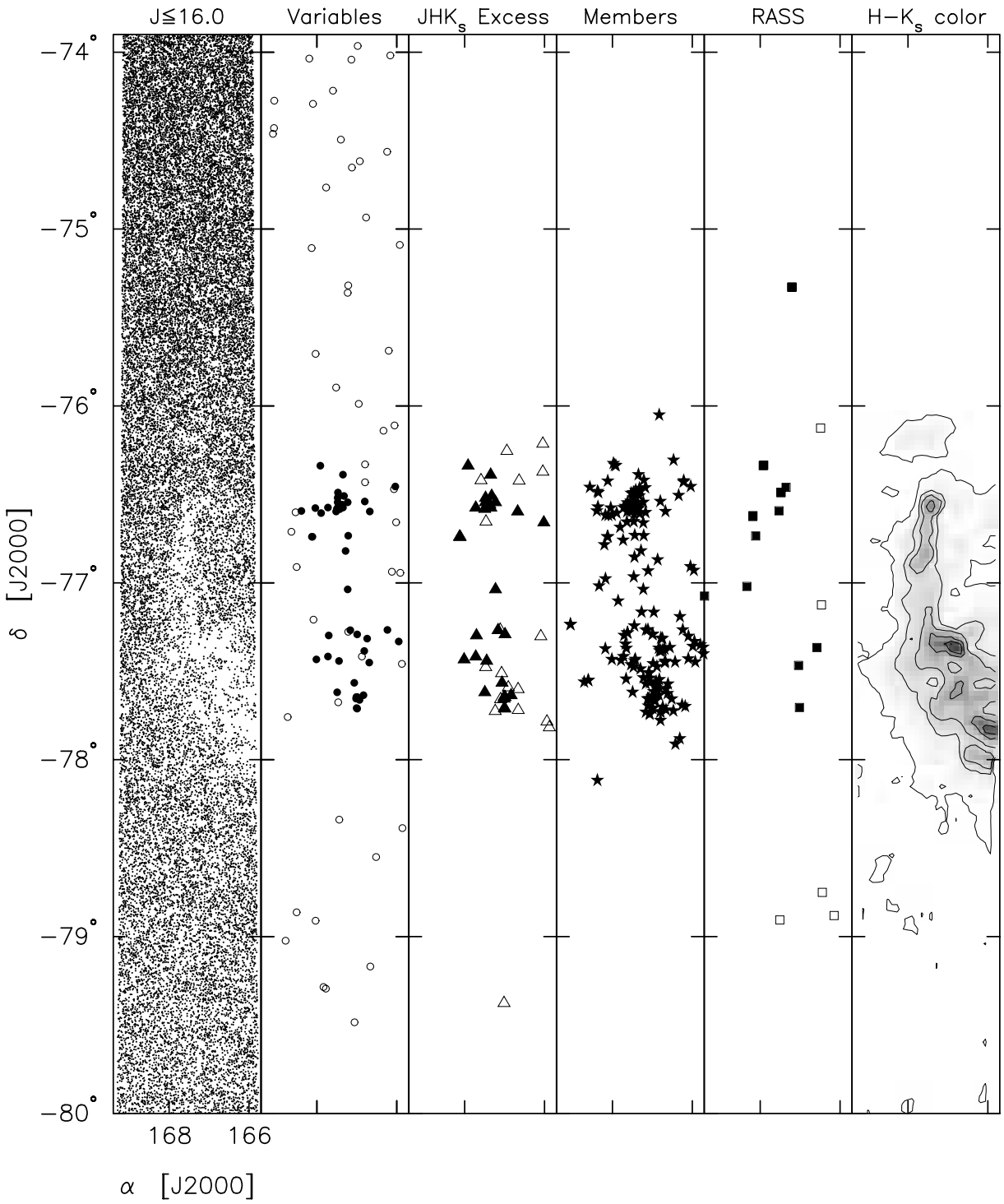

FIG. 4.—Spatial distribution of stars toward the Chamaeleon I molecular cloud. Starting with the leftmost panel, these figures show (*a*) the spatial distribution of sources with $J \leq 16$; (*b*) location of variable stars identified from our near-infrared data, where filled symbols indicate variable stars that were previously identified as Chamaeleon I members; (*c*) sources that exhibit a near-infrared excess in the $J-H$ vs. $H-K_s$ color-color diagram, where filled triangles represent variable stars and open triangles indicate nonvariables brighter than $K_s = 13.5$; (*d*) members and candidate members of the Chamaeleon I molecular cloud identified prior to this study (see Appendix); (*e*) X-ray sources selected from the *ROSAT* All-Sky Survey, where filled squares represent X-ray sources that have been associated with pre–main-sequence objects and open squares represent objects unrelated to Chamaeleon I (Alcalá et al. 1995); and (*f*) a map of the average $H-K_s$ stellar color with 5′ resolution, where the contour levels are at 0.20, 0.35, 0.50 mag, and increments of 0.30 mag thereafter. These panels show that the largest concentration of variable stars is toward the Chamaeleon I molecular cloud despite the overall decrease in the stellar surface density, indicating many of the variable stars must be associated with the Chamaeleon I molecular cloud.

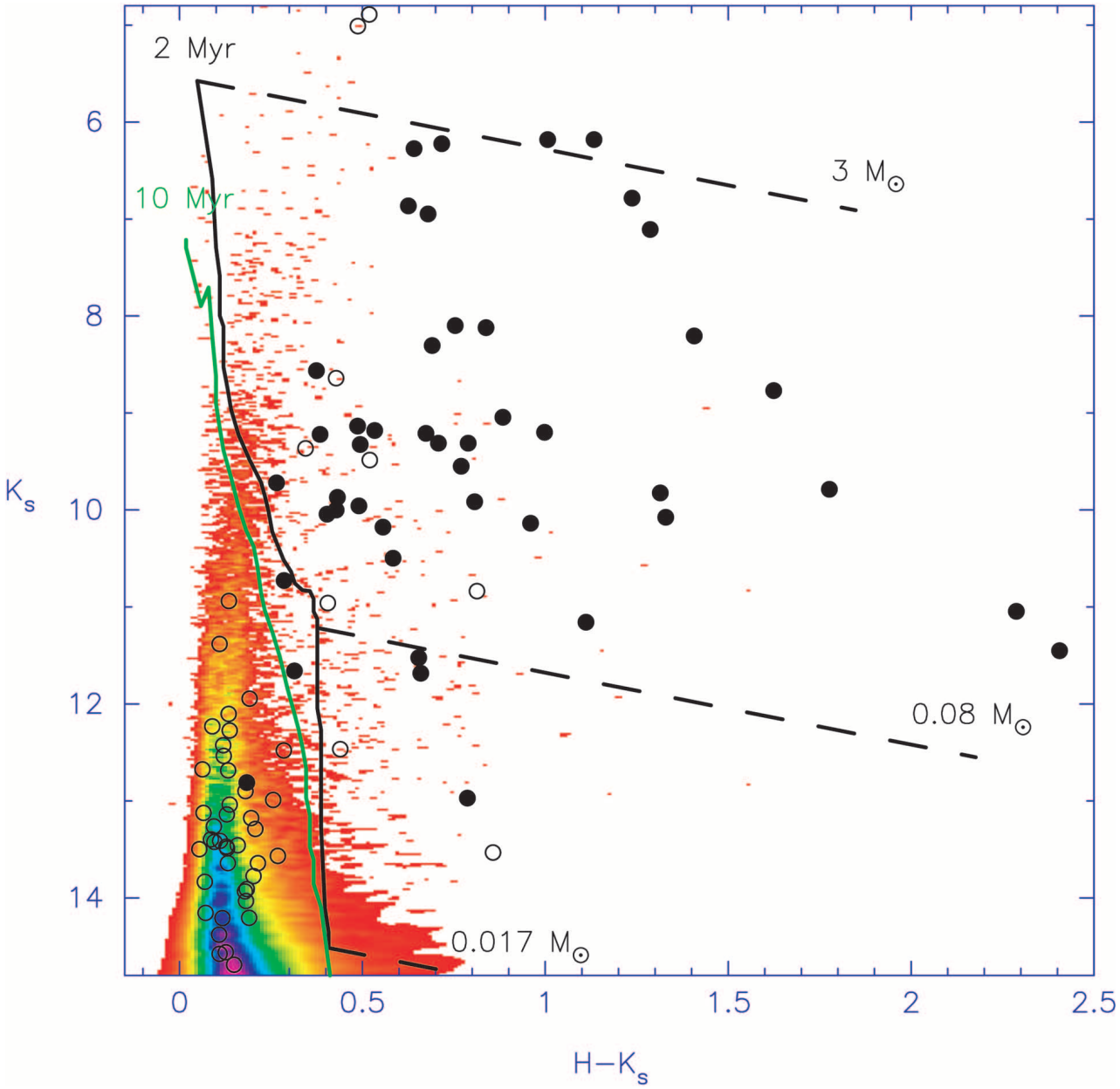

FIG. 5.—K_s vs. $H-K_s$ color-magnitude diagram for all stars (*color scale*) and the variable stars (*circles*). Filled circles indicate stars that have been previously identified as members of Chamaeleon I. The solid black curve shows the 2 Myr pre–main-sequence isochrone from D'Antona & Mazzitelli (1997, 1998) for masses between 0.017 and 3.0 $M_\odot$, and the green curve shows the 10 Myr isochrone. The dashed lines indicate the reddening vector for 10 magnitudes of visual extinction from Cohen et al. (1981) transformed into the 2MASS photometric system (Carpenter 2001), where the reddening vector is drawn at 0.017, 0.08, and 3.0 $M_\odot$. This figure shows that a large number of the variable stars are consistent with reddened pre–main-sequence stars with masses $\lesssim 3\ M_\odot$. A second group of variable stars are faint and blue and, as discussed in the text, are most likely variable field stars or old pre–main-sequence stars unrelated to Chamaeleon I.

able star of unknown type. The fourth red variable located off of the Chamaeleon I molecular cloud is anonymous.

In contrast to the red variable stars, the blue variables are found scattered over the entire 6° declination range of the survey. Figure 5 shows that, in general, these stars are too blue to be consistent with the 2 Myr old Chamaeleon I pre–main-sequence population. The blue variable stars may represent either field stars unrelated to Chamaeleon I or older pre–main-sequence stars that have formed in Chamaeleon I or its vicinity but that have since dispersed around the cloud. For example, assuming a 1 km s^{-1} velocity dispersion, a 10 Myr pre–main-sequence population at the distance of Chamaeleon I will disperse over a 3° radius region if the binding energy from the molecular cloud is negligible. We find near-infrared variables over at least 6° centered on Chamaeleon I.

To investigate whether the faint, blue variable stars could plausibly represent an older generation of stars in the vicinity of the Chamaeleon I molecular cloud, the green dotted curve in Figure 5 shows the 10 Myr pre–main-sequence isochrone. As stars and brown dwarfs evolve toward the main sequence, they become blue and fainter, but even compared to the 10 Myr old isochrone, most of faint variable stars have colors that are too blue. While it is unlikely that the

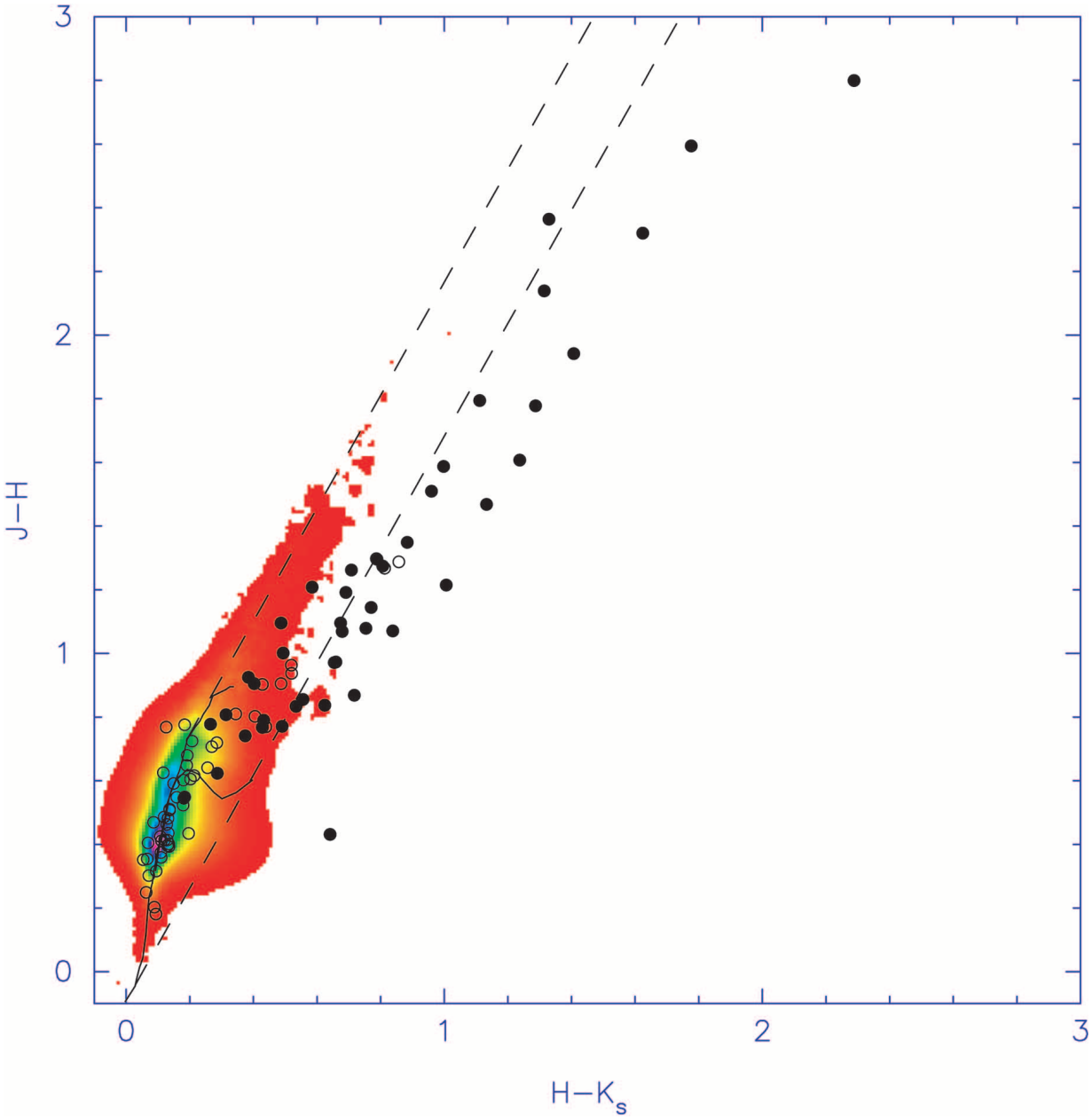

FIG. 6.—$J-H$ vs. $H-K_s$ color-color diagram for all stars (*color scale*) and the 95 variable stars (*circles*) identified from the J, H, and K_s time-series data. The filled circles represent variable stars that were previously identified as likely Chamaeleon I members.

widely distributed variables are made up of low-mass stars less than 10 Myr old, their colors and magnitudes are consistent with an older population (greater than 10 Myr) of low-mass pre–main-sequence stars (less than 1 $M_\odot$) located beyond the Chamaeleon I cloud. Such a population could have formed at the edge of an H I spur associated with Upper Sco OB association, similar to the η Cha and TW Hya associations (Mamajek & Feigelson 2001).

Alternatively, the blue variables have properties roughly expected from a main-sequence field star population in that they coincide with the peak density of field stars shown in Figure 5, exhibit a north-south gradient in their spatial distribution (see Figs. 5 and 7), and have colors consistent with G and K dwarfs (see Fig. 6). The main difficulty with this interpretation is in understanding the origin of the near-infrared variability if these are indeed old field stars. Follow-up spectroscopic observations to search for lithium in these sources will help distinguish if the widespread variable stars are field objects or a greater than 10 Myr pre–main-sequence population.

4. CANDIDATE MEMBERS OF THE CHAMAELEON I MOLECULAR CLOUD

As summarized in the Appendix, the current census of the stellar population in the Chamaeleon I molecular cloud has been established based on optical variability studies, optical spectroscopy, X-rays, and infrared surveys. The monitoring observations obtained here complement and expand these previous studies and allow candidate members to be identified based on variability in the J, H, and K_s time-series data and from near-infrared excesses in the $J-H$ versus $H-K_s$

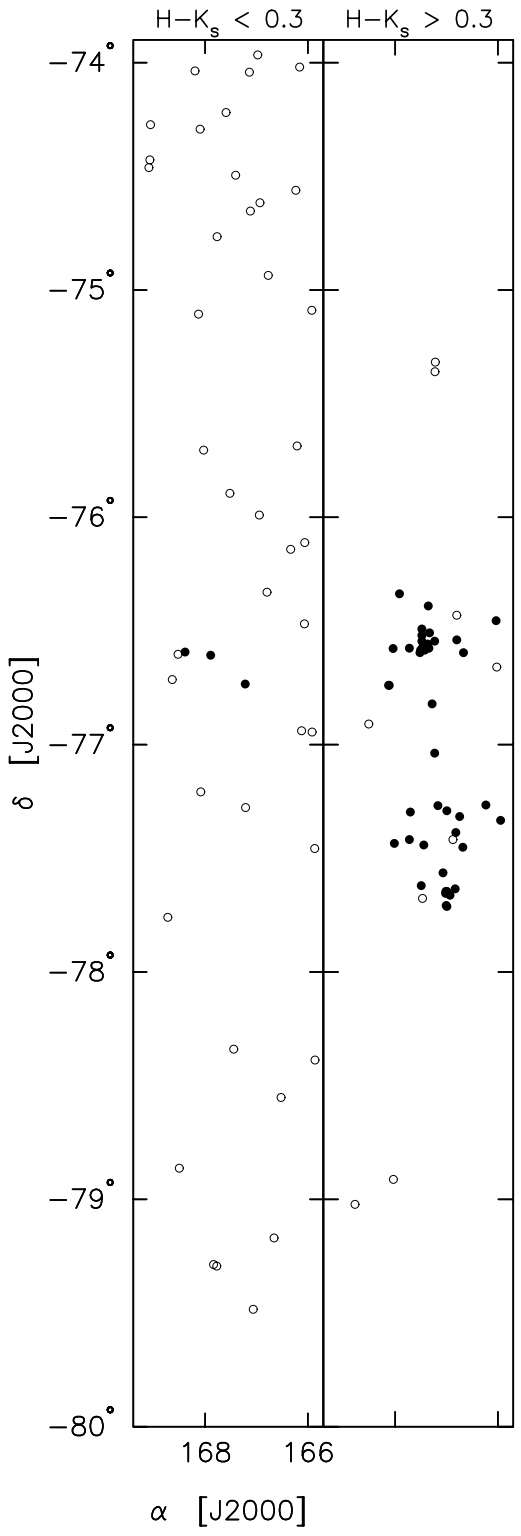

FIG. 7.—Spatial distribution of variable stars for two different color ranges. The left panel shows the distribution of relatively blue variables with $(H-K_s) < 0.3$, and the right panel shows the distribution of red variables with $(H-K_s) > 0.3$. The blue variable stars are found over the entire region, while the red variable stars, not surprisingly, are located mainly toward the molecular cloud. Of the four red variable stars found well outside the cloud boundaries, one is thought to be a Mira variable, one is a known pre–main-sequence star identified from the *ROSAT* All-Sky Survey (Alcalá et al. 1995), and the remaining two are of unknown origin. As discussed in the text, the faint, blue variable stars are most likely field stars or an older population (greater than 10 Myr) of low-mass pre–main-sequence stars located beyond the Chamaeleon I cloud.

color-color diagram. In this section, we use our infrared variability data to identify new candidate members of the Chamaeleon I association and comment on the completeness of the current stellar/substellar membership.

4.1. *Variables*

Of the 95 variable stars identified in the survey, 45 are associated with stars that have been suggested previously as members of Chamaeleon I. As discussed in § 3.4, most of the remaining 50 variable stars are likely field stars or an intermediate-age ($\gtrsim$10 Myr) pre–main-sequence population based on their colors, magnitudes, and spatial distribution. However, five variable stars have near-infrared colors $(H-K_s > 0.3)$ and coordinates $(-77.^{\circ}8 < \delta < -76.^{\circ}2)$ generally consistent with being cluster members (see Fig. 7). Of these five stars, one is YY Cha with a magnitude of $K_s = 4.891$ and is most likely a Mira variable (Whittet, Prusti, & Wesselius 1991). The remaining four stars have not been previously identified as variable stars; their identification numbers, coordinates, and photometry are summarized in Table 4. The K_s-band magnitudes of these four variables range from 10.8 to 13.5, and two objects (9484 and 15991) have K_s magnitudes and $H-K_s$ colors that imply masses below the hydrogen burning limit if they are 2 Myr old objects at the distance of Chamaeleon I. As described in the next section, two of these variable stars (1715 and 15991) also exhibit an apparent near-infrared excess in the $J-H$ versus $H-K_s$ color-color diagram, which provides additional evidence that they are likely members of the Chamaeleon I association.

4.2. *Near-infrared Excess*

Previous studies have identified candidate members of Chamaeleon I based on the presence of a near-infrared excess in a color-color diagram (Cambrésy et al. 1998; Oasa, Tamura, & Sugitani 1999; Gómez & Kenyon 2001). The angular extent of our survey and the precision that results from averaging all of the photometric measurements (typically between 12 and 25 independent observations per band per star) has produced an extensive, high signal-to-noise database of near-infrared photometry with which to conduct a more accurate census of stars with near-infrared excesses than previously possible. For the purpose of this exercise, a star was defined to have a near-infrared excess if the average colors of all photometric measurements are such that the star is located to the right of the rightmost reddening vector shown in Figure 6. This approach is sensitive to stars with large enough infrared excesses to shift the observed colors outside the reddening vector drawn from the extrema of the color range at early O and late M spectral types. Stars with smaller infrared excess cannot be distinguished from reddened field stars in this diagram. The main-sequence locus and reddening vector were adopted from Bessell & Brett (1988) and Cohen et al. (1981), respectively, and transformed into the 2MASS photometric system using the relations in Carpenter (2001). The main-sequence locus from Bessell & Brett (1988) extends to M6 spectral types. Therefore, stars located to the right of the reddening vector may signify an apparent infrared excess due to photometric noise, a true infrared excess presumably due to an optically thick inner circumstellar disk, or a spectral type later than M6 but earlier than ~L9 (Kirkpatrick et al. 2000; Leggett et al. 2002), since the T dwarfs have bluer infrared colors.

TABLE 4
NEW CANDIDATE MEMBERS OF CHAMAELEON I

	Coordinates (J2000.0)		Mean Magnitudes			Observed rms					
ID	α	δ	J	H	K_s	J	H	K_s	Variable?	JHK_s Excess?	Name
1715	166.017772	−76.659153	12.906	11.651	10.837	0.203	0.161	0.129	Yes	Yes	
1982	166.044294	−76.213627	13.141	12.522	12.125	0.016	0.044	0.015		Yes	
7869	166.636396	−76.422525	14.270	13.597	13.153	0.049	0.065	0.043		Yes	
9484	166.799142	−76.430582	13.667	12.904	12.466	0.066	0.054	0.041	Yes		
10193	166.874272	−77.417151	12.163	11.353	10.958	0.121	0.112	0.111	Yes		
10862	166.944190	−76.254861	13.972	13.031	12.374	0.045	0.047	0.040		Yes	GK 18
11564	167.014837	−79.376292	14.459	13.483	12.265	0.052	0.043	0.041		Yes	
13788	167.236477	−77.724595	15.256	13.513	12.449	0.214	0.116	0.052		Yes	Cam2 35
15991	167.468918	−77.676413	15.672	14.386	13.532	0.195	0.173	0.186	Yes	Yes	
17173	167.592793	−76.420500	13.618	12.947	12.485	0.041	0.049	0.030		Yes	

Figure 8 shows $J-H$ versus $H-K$ color-color diagrams in four different K_s-band magnitude intervals for sources with at least 10 $J-H$ and $H-K_s$ measurements. The later criteria were arbitrarily imposed to ensure high signal-to-noise photometry. Sources brighter than $K_s = 14$ and with near-infrared excess have $J-H$ colors that range between ~1 and 3 mag. Spatially, these bright sources are located toward the Chamaeleon I molecular cloud (see Fig. 4). These properties are consistent with the notion that the bright objects with infrared excesses are pre–main-sequence stars surrounded

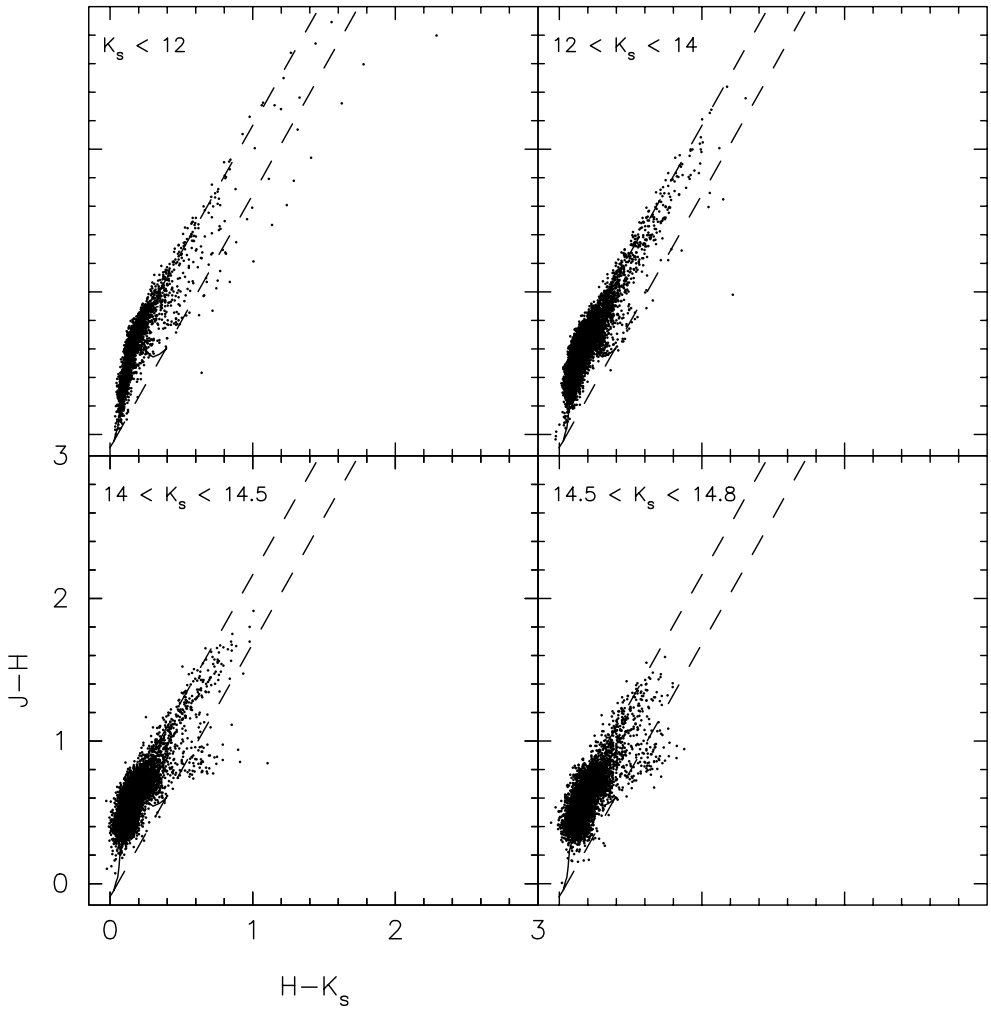

FIG. 8.—$J-H$ vs. $H-K_s$ color-color diagrams in four different K_s-band magnitude intervals for objects in the source list with at least 10 $J-H$ and $H-K_s$ measurements. The number of sources shown in each panel are 2869 for $K_s < 12$, 10,070 for $12 < K_s < 14$, 6336 for $14 < K_s < 14.5$, and 5320 for $14.5 < K_s < 14.8$. Sources with a near-infrared excess and brighter than $K_s = 14$ are most likely stars associated with Chamaeleon I and surrounded by an accretion disk. The fainter sources with an infrared excess are most likely galaxies with redshifts of $z \lesssim 0.25$, as discussed in the text.

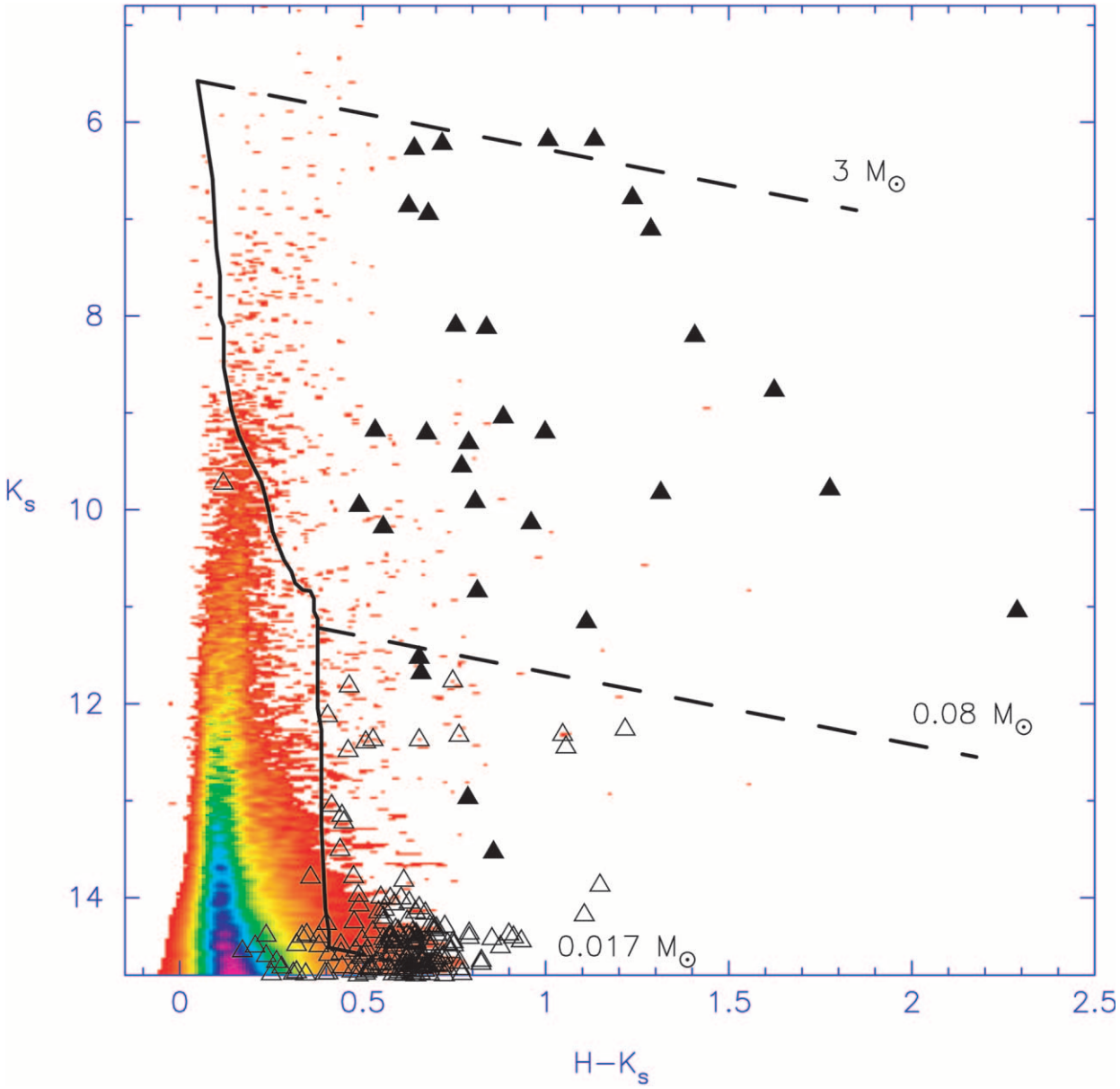

FIG. 9.—K_s vs. $H-K_s$ color-magnitude diagram for all sources (*color scale*) and sources with a near-infrared excess (*triangles*) detectable in the $J-H$ vs. $H-K_s$ color-color diagram. Filled triangles represent the subset of sources with excesses that are also variable. Sources with excesses and brighter than $K_s = 13.5$ (see Fig. 4) are clustered around the Chamaeleon I molecular cloud and are most likely pre–main-sequence stars (for $K_s \lesssim 11$) and brown dwarf candidates (for $11 \lesssim K_s \lesssim 13.5$). Objects fainter than $K_s = 13.5$ are distributed over the entire survey area and are most likely galaxies, as discussed in the text.

by optically thick accretion disks embedded within the Chamaeleon I molecular cloud.

The K_s versus $H-K_s$ color-magnitude diagram for the 208 sources with an apparent near-infrared excess is shown in Figure 9, where filled symbols denote stars with a near-infrared excess that also show infrared variability, and open symbols indicate nonvariable sources with an excess. Figure 9 shows that all but one source with a near-infrared excess and brighter than $K_s = 11.5$ (approximately the hydrogen burning limit for the distance and age of Chamaeleon I with no extinction) is also variable in the near-infrared. The one star (identification number 1959) with an apparent infrared excess and is not variable has blue infrared colors ($J-H$, $H-K_s = 0.104$, 0.120) and possesses a small near-infrared excess. The $H-K_s$ color for this star is too blue to be consistent with membership in the Chamaeleon I association assuming an age of 2 Myr. We suspect, therefore, that this star most likely has an apparent near-infrared excess due to photometric noise, and we do not list this star as a candidate member of Chamaeleon I.

Figures 8 and 9 also show a population of 155 sources fainter than $K_s = 14$ that, if stellar, exhibit a near-infrared excess. From visual inspection of the images, a few of these sources have suspect photometry due to a nearby bright star or a close companion. However, for most of the objects, there is no a priori reason to question the photometry. The apparent excesses cannot be attributed to random photometric noise, since one would expect that these objects would be present with colors ranging from $(J-H) = 0.3$ to 0.9, where the stellar density is highest in the color-color

plot. Instead, most of the faint objects with excesses are found in a narrow range of colors between $(J-H) = 0.8$ and 1.0. Spatially, these objects are found over the full 6° declination range of the survey. While we cannot exclude the possibility that these objects are very low mass objects dispersed from Chamaeleon I, such a scenario would seem unlikely, since it would require disparate spatial distributions between the substellar and the stellar populations and would imply that the Chamaeleon I initial mass function (IMF) is heavily weighted toward brown dwarf objects in contrast to the IMF in other nearby star-forming regions (see, e.g., Luhman et al. 2000). The faint infrared-excess objects cannot be field brown dwarfs, since their surface density of $\sim$15 deg^{-2} between $K_s = 14$ and 14.5 is $\sim$300 times larger than the surface density of L dwarfs down to $K_s = 14.5$ (Kirkpatrick et al. 1999).

The remaining possibility then is that the faint sources with near-infrared excesses are galaxies, where the recessional velocities shift the galaxy colors to the right of the reddening vector in the $J-H$ versus $H-K_s$ diagram. The near-infrared colors observed in Figure 8 can be accounted for by a population of galaxies at redshifts between $\sim$0.1 and 0.25 (Mannucci et al. 2001). Photometric and spectroscopic surveys have, in fact, shown that galaxies with magnitudes of $K = 14$–15 have a mean redshift of 0.18 (Songaila et al. 1994) and a surface density of $\sim$100 deg^{-2} (Väisänen et al. 2000). By comparison, the observed surface density of sources in Chamaeleon I with near-infrared excesses and fainter than $K_s = 14$ is $\sim$35 deg^{-2}. The lower surface density of faint near-infrared–excess sources compared with the expected galaxy population may be attributed to the high extinction from the Chamaeleon I molecular cloud and not all of the galaxies will have high enough redshift to produce the red near-infrared colors. We therefore conclude that the sources with a near-infrared excess and fainter than $K_s = 14$ consist predominantly of galaxies with redshifts of $\sim$0.2.

Given the apparent predominance of galaxies among the near-infrared–excess objects at faint magnitudes, we only considered infrared-excess sources brighter than $K_s = 13.5$ as possible members of Chamaeleon I. The spatial distribution of these 45 objects is shown in the third panel of Figure 4. All but one is concentrated toward the cloud. The one exception, star 11564 in our source list (J2000.0 equatorial coordinates of α, $\delta = 11^{\rm h}08^{\rm m}03\overset{\rm s}{.}56$, $-79°22'34\overset{''}{.}65$), has average colors of $(J-H) = 0.976$ and $(H-K_s) = 1.218$. The infrared excess appears in each of the 24 individual photometric measurements with a PSF χ^2 less than two in all observations. Therefore, the near-infrared excess cannot be merely because of photometric noise or a poor PSF fit. This object may either be an isolated young star with near-infrared excess or a bright, red galaxy. We interpret the remainder of the near-infrared–excess sources brighter than $K_s = 13.5$ as young stellar objects whose excesses can be accounted for by an optically thick inner circumstellar disk for the brighter objects and/or a spectral type later than $\sim$M6 for the fainter objects. Table 4 lists the seven new near-infrared candidates members identified from our observations that are located in the vicinity of the Chamaeleon I molecular cloud. (The eighth star with an infrared excess in Table 4 is fainter than our imposed magnitude limit but is included in the table as a candidate members because it is a variable.)

We note that we did not confirm many of the near-infrared–excess stars identified in previous studies. Cambrésy et al. (1998) selected 54 candidate members in Chamaeleon I based on near-infrared excess in the $I-J$ versus $J-K$ diagram or redder colors than expected from a Chamaeleon I extinction map. Of these 54 stars, 42 are in our database with three-band photometry, and only six show an infrared excess in our data. One of these sources is identified in Table 4, and three others (identification numbers 32, 41, and 49 in Table 2 of Cambresy et al. 1998) are indicated as candidate members in the Appendix, since they have other characteristics that suggest they may be pre–main-sequence stars. The remaining two sources (identification numbers 329 and 926 in our study and 10 and 11, respectively, in Cambresy et al. 1998) show infrared excess in our data as well, but they were detected on only 5–6 J-band images because of the faintness of the object and were not included in the near-infrared–excess analysis. Similarly, Gómez & Kenyon (2001) list 56 infrared-excess candidates (identified from the $J-H$ vs. $H-K_s$ diagram) brighter than $K_s = 14$, of which 49 are three-band detections in our observations. Only seven of these sources show an infrared excess. One of these objects is indicated in Table 4, four others (identification numbers 13, 29, 30, and 31 in Gómez & Kenyon 2001) are listed in the Appendix as members based on other studies, and two (identification numbers 10 and 40 in Gómez & Kenyon 2001) are fainter than $K_s = 14$ in our study and did not meet our magnitude criterion. (As shown in CHS01, some stars do show a transient near-infrared excess. However, it is unlikely that this can account for the majority of the Gómez & Kenyon sources, since an equally large number of new near-infrared excesses should have been identified in our observations, which is not observed.) Finally, Oasa et al. (1999) list 19 sources with infrared excesses, of which 12 are in our database. The remaining seven sources are fainter than our sensitivity limits. Of these 12 sources, seven show an infrared excess. All of the infrared-excess candidates from Oasa et al. (1999) are listed in the Appendix.

4.3. *Discussion*

The area covered by our observations encompasses 170 known or candidate Chamaeleon I members identified prior to this study, of which 159 have been detected in the near-infrared with our data. As discussed in CHS01, the monitoring observations discussed here are most sensitive to detecting variables brighter than $K_s \sim 12$. Of the 129 Chamaeleon I members brighter than this limit, 43, or 33%, have been detected as variable. The variables include stars with and without near-infrared excesses as traced in the $J-H$ versus $H-K_s$ diagram, although the variability observations are biased toward detecting stars with excesses. That is, of the Chamaeleon I members brighter than $K_s = 12$, 23% (30/129) have a near-infrared excess, but 28/43 (65%) of the variables have an excess. Thus, the proportion of bright stars that have a near-infrared excess is higher among the variable compared with the Chamaeleon I members at a $\sim$5 σ confidence level. Similarly, in Orion, 19% ± 1% of the stars brighter than $K_s = 12$ exhibit a near-infrared excess, compared with 28% ± 2% of the variables brighter than this limit. While the Orion variables are also slightly biased toward stars with infrared excesses (at the $\sim$4.5 σ confidence level), the bias is not as strong, in that the overall percentage of variables with an infrared excess is lower in Orion by a factor of 2.3 ± 0.3.

The fact that nearly all Chamaeleon I members with a near-infrared excess and brighter than $K_s = 12$ are also variable suggests that the variability may be related to the presence of an inner accretion disk. Further evidence for this conjecture comes from the type of variability exhibited by stars with infrared excesses. Of the 14 stars in Chamaeleon I that show measurable color variability, where the stellar color becomes redder as the star fades (see § 3.2), 12 have a near-infrared excess. These near-infrared color variations cannot be readily accounted for by cool spots on the stellar surface (Skrutskie et al. 1996; CHS01). They can, however, be explained by extinction variations (perhaps from a warped circumstellar disk) or hot spots on the stellar surface produced by accretion from the disk onto the star. However, hot spots can only produce colors variations of up to $\sim$0.1 mag in the near-infrared given typical hot spot parameters modeled in T Tauri stars, and extinction variations may be the preferred explanation for the large amplitude variables (see CHS01). More extensive observations and modeling of these color variations may provide a unique window into the properties of the inner circumstellar disk.

Two of the Chamaeleon I variables (identification numbers 18416 and 21473) that show color variations have masses near the hydrogen burning limit as inferred from the K_s versus $H-K_s$ diagram. This suggests that the variability mechanisms discussed in context of the Orion observations for stars more massive than 1 $M_\odot$ may extend to lower mass objects. For fainter sources between K_s magnitudes of 12.0 to 13.5, and presumably lower mass, only 8% (1/13) of the near-infrared–excess objects also show variability. The lack of variability in these sources does not necessarily imply a change in the infrared-excess–variability relation for substellar objects, however. Not only are these observations less sensitive to variability for sources fainter than $K_s = 12$, but the apparent infrared excess may be due to a spectral type later than M6 and not to a circumstellar disk.

Finally, we briefly discuss the implication of these observations for the current census of the stellar and substellar population in Chamaeleon I. The region we surveyed contains 129 known or candidate Chamaeleon I members brighter than $K_s = 12$. Only two new candidate members brighter than $K_s = 12$ have been identified in this study from either variability or a near-infrared excess. Since nearly all bright objects with a near-infrared excess are also variable, these observations suggest that the current census of Chamaeleon I sources is nearly complete for objects brighter than $K_s = 12$ and with an infrared excess in the $J-H$ versus $H-K_s$ diagram. Comerón, Neuhäuser, & Kaas (2000) recently identified 13 low-mass stars and brown dwarfs in Chamaeleon I from an Hα prism survey. Nine of these sources have magnitudes of $10.6 < K_s < 12$, but none were detected as variable, and only one was identified as distinctive in this data set because of an apparent infrared excess. The other four sources in Comerón et al. (2000) are fainter than $K_s = 12$, and interestingly three were identified here as having a near-infrared excess, where the excess for these objects may be due to a late spectral type. While the statistics are small, the comparison with Comerón et al. (2000) suggests that the $J-H$ versus $H-K_s$ diagram is fairly efficient at identifying the substellar objects. The fact that only eight new candidate members were identified with magnitudes of $12 < K_s < 13.5$ suggests brown dwarfs will not substantially expand the current population census of Chamaeleon I.

5. SUMMARY

We have conducted a J, H, and K_s variability study of stars in a $0\overset{\circ}{.}72 \times 6^\circ$ region centered on the Chamaeleon I molecular cloud and T association. Observations were obtained on two nights in 2000 January and 13 nights in 2000 April and May using the 2MASS south telescope. Compared with our variability study of the Orion A molecular cloud (CHS01), which was sensitive to variable stars more massive than $\sim$1 $M_\odot$, observations of the closer Chamaeleon I star-forming region permit variability to be detected in lower mass stars and brown dwarfs down to $\sim$0.05 $M_\odot$.

Of the 34,539 sources meeting the photometric completeness criteria, 95 have been identified as variable from either a large Stetson (1996) variability index or a large reduced χ^2 in the time-series data. The variables can be coarsely grouped into a population of bright ($K_s < 12$), red ($H-K_s > 0.3$) stars and a population of faint ($K_s > 12$), blue ($H-K_s < 0.3$) stars. Most of the "red" variables are known members of the Chamaeleon I association and, as expected, have near-infrared colors and magnitudes consistent with a young, pre–main-sequence population. The "blue" variables are distributed over the full 6° of the survey area. The colors and magnitudes of the blue variables are inconsistent with a pre–main-sequence population as old as 10 Myr at the distance of Chamaeleon I but can be explained as a population of older pre–main-sequence stars unrelated to Chamaeleon I or variable field stars.

The time-series data were used to identify new candidate members of the Chamaeleon I association that show photometric variability and/or a near-infrared–excess characteristics of an optically thick circumstellar disk. Of the 95 variables identified in this study, 45 were known prior to this study as members or candidate members of Chamaeleon I. Among the remaining 50 variables, we have identified four new sources that have colors and coordinates consistent with low-mass, pre–main-sequence members of the Chamaeleon I association. A total of 208 sources brighter than $K_s = 14.8$ were identified as having a near-infrared excess in the $J-H$ versus $H-K_s$ color-color diagram. The fainter sources with near-infrared excesses ($K_s < 14$) are randomly distributed over the 6° survey region. Based on their spatial distribution, location in the color-color diagram, and surface density, we suggest that these objects are most likely galaxies with redshifts of $z \lesssim 0.25$. The 45 sources brighter than $K_s = 13.5$ and with infrared excesses are clustered spatially around the Chamaeleon I molecular cloud and are likely association members. Seven of these relatively bright sources with excesses are new candidate members of Chamaeleon I, including one that is also variable. In total, 10 new candidate members have been identified, eight of which have colors and magnitudes consistent with young brown dwarfs at the distance of Chamaeleon I. These observations suggest that the current census of the Chamaeleon I population is complete for objects brighter than $K_s = 12$ and with a near-infrared excess in the $J-H$ versus $H-K_s$ diagram.

As a product of this study, these observations have yielded a precise data set of photometry and astrometry for previously identified Chamaeleon I members. In the Appendix, we summarize the J, H, and K_s magnitudes and cross-identifications for Chamaeleon I members.

We would like to thank the 2MASS observatory staff and the data management team for acquiring and pipeline processing the special survey observations used in this investigation. This publication makes use of data products from the Two Micron All Sky Survey, which is a joint project of the University of Massachusetts and the Infrared Processing and Analysis Center, funded by the National Aeronautics and Space Administration and the National Science Foundation. The 2MASS science data and information services were provided by the InfraRed Science Archive at IPAC. This research has made use of the SIMBAD database, operated at CDS, Strasbourg, France. J. M. C. acknowledges support from Long Term Space Astrophysics Grant NAG 5-8217 and the Owens Valley Radio Observatory, which is supported by the National Science Foundation through grant AST 99-81546.

APPENDIX A

ASTROMETRY AND PHOTOMETRY FOR PREVIOUSLY IDENTIFIED MEMBERS OF CHAMAELEON I

During the course of this study, a membership list for Chamaeleon I was compiled using published observations. This Appendix presents the compilation of known and candidate members of the Chamaeleon I association and summarizes the astrometry and J, H, and K_s photometry obtained from our observations.

The Chamaeleon I association was initially identified as a spatial concentration of optical variable stars (Hoffmeister 1962). Subsequent studies expanded the association membership through objective prism or CCD Hα emission-line surveys (Henize & Mendoza 1973; Schwartz 1977; Hartigan 1993) and spectroscopic follow-up of individual stars (Appenzeller 1977, 1979; Rydgren 1980; Appenzeller, Jankovics, & Krautter 1983) to identify stars with spectral features characteristic of pre–main-sequence objects. More recent objective prism surveys, followed by spectroscopic observations and multiwavelength imaging, have begun to probe the Chamaeleon I population in the substellar regime (Comerón, Rieke, & Neuhäuser 1999; Comerón et al. 2000). Additional pre–main-sequence candidates have been identified in X-rays from *Einstein* (Feigelson & Kriss 1989) and *ROSAT* (Feigelson et al. 1993; Alcalá et al. 1995), where pre–main-sequence counterparts to the X-ray sources have been identified from optical spectroscopic follow-up observations (Walter 1992; Huenemoerder, Lawson, & Feigelson 1994; Alcalá et al. 1995; Lawson et al. 1996). Candidate cloud members that remain deeply embedded in the cloud have been identified from the presence of excess near-infrared emission (Hyland, Jones, & Mitchell 1982; Jones et al. 1985; Cambrésy et al. 1998; Oasa et al. 1999; Gómez & Kenyon 2001), red far-infrared colors from *IRAS* (Baud et al. 1984; Assendorp et al. 1990; Prusti et al. 1991; Whittet et al. 1991; Gauvin & Strom 1992), and more recently, red mid-infrared colors from *ISO* (Nordh et al. 1996; Persi et al. 2000; Lehtinen et al. 2001). In total, the candidate members identified by infrared excesses can more than double the known stellar population.

Table 5 summarizes the status of the stellar and substellar membership in the Chamaeleon I molecular cloud prior to this study. We include in Table 5 stars that are optically variable or show Hα emission as summarized by Whittet et al. (1987) and references therein for pre-1987 observations, the Hα objects and red stars from Hartigan (1993), the brown dwarfs from Comerón et al. (2000), candidate members identified from *IRAS* (Baud et al. 1984; Whittet et al. 1991) and *ISO* (Persi et al. 2000), and optical counterparts to X-ray sources that have spectroscopic signatures of pre–main-sequence stars (Walter 1992; Lawson et al. 1996). Table 5 also included possible deeply embedded members of Chamaeleon I that have recently been identified by the presence of excessed near-infrared (Oasa et al. 1999) and mid-infrared emission (Persi et al. 2000). Cambrésy et al. (1998) and Gómez & Kenyon (2001) have also identified $\sim$150 candidate members based on the presence of near-infrared–excess emission (and, in the case Cambresy et al. 1998, red sources without necessarily an infrared excess). Since the majority of the near-infrared–excess candidates could not be confirmed with our data (see § 4.2), these objects are not listed in Table 5 unless that star contains other characteristics indicating it is a pre–main-sequence object (see also Table 4).

Column (1) in Table 5 lists the commonly adopted name of the Chamaeleon I members. Because of the multitude of observations of the Chamaeleon I region, many of the sources have been observed as part of several studies, and the cross identifications of the various names are provided in Table 6. Most of the cross identifications were made by matching the coordinates in the original references. Two notable exceptions are that the positions for sources in the General Catalog of Variable Stars were taken from López & Girard (1990) when possible, and the association of *IRAS* sources from Baud et al. (1984) were taken from Lawson et al. (1996). Columns (2) and (3) list the J2000.0 equatorial coordinates, where the coordinates have been obtained from, in order of preference, (1) this study, (2) the 2MASS Working Database (Version 2 processing) for stars outside our survey coverage, and (3) the literature. The coordinates listed in Oasa et al. (1999) were found to differ from 2MASS by up to 10″. For sources detected only by Oasa et al. (1999), an astrometric correction was applied based on nearby sources detected both by our observations and Oasa et al. (1999). Columns (4)–(12) list the mean J, H, and K_s magnitudes, photometric rms, and number of measurements. Column (13) lists the Stetson variability index derived from our data. The 2MASS photometry for Chamaeleon I members located outside our survey boundaries have been obtained from the Version 2 2MASS Working Database. These sources can be identified in Table 5 as having no Stetson index and with $N \leq = 1$ in each band. The rms in such instances represent the photometric uncertainty from the 2MASS data reduction pipeline excluding zero-point calibration uncertainties, which are typically $\sim$1% in each band.

As noted by Schwartz (1991), many of the sources are only suspected members of the cloud and have yet to be verified spectroscopically to be pre–main-sequence stars. In particular, some stars have been identified as Chamaeleon I members because they are variable or have red photometric colors (but without an infrared excess), but no additional evidence has been obtained to indicate these are not simply field stars. Accordingly, the flags in Column (11) indicate the properties associated with each source that suggests it is a pre–main-sequence object. The flags indicate, in order

TABLE 5

NEAR-INFRARED PHOTOMETRY FOR PREVIOUSLY IDENTIFIED CHAMAELEON I MEMBERS

NAME (1)	α (J2000.0) (2)	δ (J2000.0) (3)	MEAN MAGNITUDES[a] J (4)	H (5)	K_s (6)	RMS[a] J (7)	H (8)	K_s (9)	N J (10)	H (11)	K_s (12)	VARIABILITY INDEX (13)	YSO PROPERTIES[b] (14)
T1	10 52 01.30	−77 09 50.1	13.942	13.333	13.112	0.027	0.037	0.037	1	1	1	...	0Y0 0 0 0
IRAS 10529−7638	10 54 11.6	−76 54 33	...	...	...	...	...	...	...	...	...	...	0 0 0 0 0Y
T2	10 54 13.32	−77 55 09.2	12.251	11.699	11.477	0.023	0.026	0.029	1	1	1	...	Y0 0 0 0 0
T3	10 55 59.9	−77 24 38	...	...	...	...	...	...	...	...	...	...	YY0 0 0Y
T4	10 56 30.43	−77 11 39.4	9.966	9.078	8.629	0.021	0.026	0.027	1	1	1	...	YY0Y 0Y
T5	10 57 42.28	−76 59 35.7	10.431	9.496	9.196	0.022	0.026	0.025	1	1	1	...	0Y0 0 0
CHXR 3	10 58 05.61	−77 28 24.0	8.507	7.675	7.392	0.025	0.034	0.023	1	1	1	...	0Y0Y 0Y
T6	10 58 16.84	−77 17 17.1	9.270	8.414	7.783	0.025	0.037	0.026	1	1	1	...	YY0Y 0Y
T7	10 59 01.15	−77 22 40.7	10.146	9.208	8.620	0.023	0.027	0.026	1	1	1	...	YY0Y 0Y
T8	10 59 07.00	−77 01 40.1	8.444	7.760	7.351	0.019	0.040	0.014	1	1	1	...	0Y0Y 0Y
T9	11 00 14.08	−76 44 15.4	8.855	7.880	7.363	0.011	0.034	0.023	1	1	1	...	0Y0 0 0Y
CHXR 8	11 00 14.54	−77 14 38.0	10.062	9.750	9.655	0.028	0.027	0.026	1	1	1	...	0 0 ? Y 0Y
T10	11 00 40.27	−76 19 28.0	11.848	11.242	10.851	0.026	0.026	0.026	1	1	1	...	0Y0 0 0 0
CHXR 9C	11 01 18.77	−76 27 02.5	10.032	9.303	9.024	0.027	0.027	0.026	1	1	1	...	0YYY0 0
B23	11 01 46.6	−77 43 51	...	...	...	...	...	...	...	...	...	...	0 0 0 0 0Y
B9	11 02 15.4	−77 10 59	...	...	...	...	...	...	...	...	...	...	0 0 0 0 0Y
ISO 1	11 02 16.3	−77 46 30	...	...	...	...	...	...	...	...	...	...	0 0 0 0 Y0
T11	11 02 24.92	−77 33 35.8	9.094	8.417	8.232	0.020	0.026	0.016	1	1	1	...	YY0Y YY
CHXR 71	11 02 32.67	−77 29 13.0	11.230	10.422	10.076	0.027	0.026	0.024	1	1	1	...	0Y ? Y YY
ISO 13	11 02 53.1	−77 24 07	...	...	...	...	...	...	...	...	...	...	0 0 0 0 Y0
T12	11 02 55.06	−77 21 50.9	11.559	10.847	10.449	0.027	0.026	0.026	1	1	1	...	0Y0 0 0 0
CHXR 11	11 03 11.61	−77 21 04.3	8.156	7.474	7.253	0.021	0.036	0.008	1	1	1	...	0 0 ? Y 0Y
ISO 28	11 03 41.85	−77 26 52.1	12.921	12.111	11.646	0.026	0.033	0.026	13	13	13	0.04	0 0 0 0 Y0
Hn 2	11 03 47.66	−77 19 56.4	11.353	10.449	10.044	0.044	0.051	0.048	13	13	13	1.27	YY0 0 0Y
T13	11 03 51.01	−76 55 45.6	14.374	14.049	13.942	0.067	0.052	0.062	13	13	13	0.30	Y0 0 0 0 0
CHXR 12	11 03 56.83	−77 21 33.0	10.776	10.001	9.709	0.022	0.033	0.023	13	13	13	0.33	0YYY0Y
T14	11 04 09.11	−76 27 19.3	9.668	8.935	8.563	0.056	0.063	0.067	13	13	13	1.47	YY0Y 0Y
CHXR 72	11 04 11.06	−76 54 32.2	11.845	11.174	10.959	0.031	0.025	0.024	13	13	12	0.25	0Y0Y 0 0
T14a	11 04 22.78	−77 18 08.2	14.335	13.154	12.253	0.066	0.069	0.038	11	9	9	0.53	0 0 0 0 YY
T15	11 04 24.26	−77 25 48.8	10.980	10.069	9.589	0.025	0.028	0.028	12	12	12	0.19	0Y0 0 0 0
ISO 52	11 04 42.59	−77 41 57.1	11.793	11.022	10.621	0.023	0.019	0.037	12	12	11	0.06	0 0 0 0 YY
CHXR 14N	11 04 51.03	−76 25 24.0	10.535	9.822	9.604	0.025	0.029	0.019	12	12	12	0.36	0YYY 0 0
CHXR 14S	11 04 52.87	−76 25 51.5	10.695	9.931	9.716	0.031	0.033	0.028	12	12	12	0.83	0YYY 0 0
T16	11 04 57.00	−77 15 57.0	12.245	10.974	10.498	0.448	0.296	0.359	16	16	17	7.83	YY0 0 YY
B29	11 05 01.9	−77 41 31	...	...	...	...	...	...	...	...	...	...	0 0 0 0 0Y
Hn 4	11 05 14.64	−77 11 29.2	10.913	9.976	9.590	0.025	0.026	0.023	24	24	22	0.30	0Y0 0 0 0
T18	11 05 15.23	−77 52 54.7	13.054	11.912	11.475	0.031	0.024	0.031	25	25	25	0.28	0Y0 0 0 0
T17	11 05 21.60	−76 30 21.6	13.254	12.781	12.653	0.032	0.033	0.037	24	24	24	0.08	Y0 0 0 0 0
T19	11 05 41.57	−77 54 44.0	11.346	10.752	10.598	0.020	0.030	0.020	25	25	24	0.10	0Y0 0 0 0
CHXR 15	11 05 42.97	−77 26 51.7	11.216	10.555	10.208	0.023	0.032	0.032	24	24	23	0.44	0Y0Y 0Y
T20	11 05 52.62	−76 18 25.5	10.249	9.543	9.311	0.032	0.038	0.031	12	12	12	0.78	YY0Y 0 0
ISO 68	11 05 53.93	−77 43 27.2	13.464	12.372	11.896	0.038	0.032	0.034	21	23	22	0.47	0 0 0 0 Y0
ISO 71	11 06 04.06	−77 39 23.8	15.309	13.621	12.915	0.065	0.039	0.026	12	12	12	0.10	0 0 0 0 Y0
T21	11 06 15.36	−77 21 56.7	7.614	6.811	6.445	0.016	0.021	0.012	12	12	12	0.26	0YYYY
B31	11 06 26.4	−77 34 20	...	...	...	...	...	...	...	...	...	...	0 0 0 0 0Y
CHXR 73	11 06 28.72	−77 37 33.2	12.628	11.269	10.689	0.045	0.025	0.031	22	21	21	0.41	0 0 0Y 0Y
Cha Ha 12	11 06 37.93	−77 43 09.2	12.997	12.281	11.818	0.038	0.032	0.027	24	24	24	0.31	0Y0 0 Y0
ISO 79	11 06 39.42	−77 36 05.3	14.962	13.367	12.321	0.064	0.050	0.039	23	23	23	0.57	0 0 0 0 Y0
Hn 5	11 06 41.76	−76 35 49.2	11.588	10.727	10.177	0.072	0.059	0.039	24	24	24	1.19	YY0 0 Y0
T22	11 06 43.43	−77 26 34.5	10.753	9.718	9.347	0.033	0.033	0.031	24	24	24	0.46	Y0 0 0 0 0
CHXR 20	11 06 45.05	−77 27 02.5	10.717	9.628	9.134	0.617	0.458	0.334	24	24	24	12.42	YYYYYY
Ced 110 IRS4	11 06 46.23	−77 22 29.0	...	15.337	...	...	0.126	0.244	...	6	...	−0.52	0 0 0 0 0Y
CHXR 74	11 06 57.29	−77 42 10.6	11.431	10.589	10.217	0.032	0.038	0.023	23	23	22	0.15	0Y ? Y0Y
ISO 86	11 06 58.01	−77 22 48.8	...	...	13.458	...	...	0.095	...	...	24	0.90	0 0 0 0 Y0
T23	11 06 59.01	−77 18 53.5	11.195	10.429	9.999	0.044	0.051	0.049	24	23	23	1.20	YY0 0YY
Ced 110 IRS6	11 07 09.15	−77 23 05.0	...	14.747	11.010	...	0.097	0.056	...	24	21	0.41	0 0 0 0YY
ISO 91	11 07 09.19	−77 18 47.1	14.912	12.602	11.445	0.046	0.031	0.035	24	23	23	0.23	0 0 0 0 Y 0
CHXR 22W	11 07 10.42	−77 43 44.2	14.042	12.975	12.455	0.030	0.037	0.037	24	24	24	0.06	0 0 0YY 0
CHXR 21	11 07 11.43	−77 46 39.4	11.077	10.024	9.621	0.016	0.029	0.024	24	24	23	0.09	0Y ? Y0Y
T24	11 07 12.04	−76 32 23.3	10.829	9.837	9.325	0.170	0.145	0.088	24	24	22	3.63	YY0Y 0 0
CHXR 22E	11 07 13.27	−77 43 49.8	11.869	10.558	9.987	0.028	0.036	0.036	24	24	24	0.44	0 0 0Y 0Y
ISO 97	11 07 16.19	−77 23 06.9	...	13.841	11.451	...	0.134	0.102	...	24	24	1.58	Y0 0 0Y 0

TABLE 5—*Continued*

Name	α (J2000.0)	δ (J2000.0)	Mean Magnitudes[a]			rms[a]			N			Variability Index	YSO Properties[b]
			J	H	K_s	J	H	K_s	J	H	K_s		
(1)	(2)	(3)	(4)	(5)	(6)	(7)	(8)	(9)	(10)	(11)	(12)	(13)	(14)
Cha Ha 1	11 07 16.65	−77 35 53.3	13.356	12.643	12.194	0.027	0.023	0.027	23	23	23	0.16	0Y0 0Y0
Cha Ha 9	11 07 18.56	−77 32 51.6	13.754	12.481	11.761	0.034	0.037	0.025	23	23	23	0.14	0Y0 0Y0
T25	11 07 19.15	−76 03 04.9	10.962	10.090	9.808	0.047	0.049	0.040	22	23	19	0.91	0Y0 0 0Y
T26	11 07 20.72	−77 38 07.3	7.810	6.941	6.224	0.021	0.034	0.040	23	23	23	0.74	YYYYYY
B35	11 07 21.38	−77 22 11.8	15.283	12.396	10.835	0.059	0.048	0.045	24	24	22	0.38	0 0 0 0YY
T27	11 07 28.24	−76 52 11.9	10.686	9.911	9.580	0.030	0.024	0.035	12	14	12	0.39	YY0Y0 0
CHXR 25	11 07 32.97	−77 28 27.9	11.644	11.032	10.783	0.023	0.023	0.024	12	12	12	0.29	0Y0Y0Y
CHXR 76	11 07 35.16	−77 34 49.5	12.144	11.246	10.892	0.046	0.040	0.038	12	12	12	0.70	0Y0Y0Y
CHXR 26	11 07 36.84	−77 33 33.6	11.618	10.043	9.337	0.054	0.053	0.039	12	8	11	0.65	0 0 0Y0Y
Cha Ha 7	11 07 37.72	−77 35 31.0	13.686	12.903	12.395	0.037	0.027	0.026	12	12	12	0.15	0Y0 0Y0
Cha Ha 2	11 07 42.44	−77 33 59.6	12.218	11.209	10.645	0.023	0.026	0.023	12	12	12	0.06	0Y0 0Y0
T28	11 07 43.64	−77 39 41.2	10.196	9.013	8.304	0.043	0.049	0.058	11	11	10	1.20	YY0YYY
Cha Ha 8	11 07 46.07	−77 40 09.0	12.813	12.008	11.530	0.026	0.043	0.021	11	11	11	0.39	0Y0 0 0 0
ISO 114	11 07 51.15	−77 10 00.1	13.933	13.282	13.084	0.032	0.052	0.038	12	12	12	−0.09	0 0 0 0Y0
Cha Ha 3	11 07 52.24	−77 36 57.2	12.346	11.571	11.120	0.031	0.037	0.025	11	11	11	0.43	0Y0 0 0 0
CHXR 28	11 07 55.85	−77 27 25.9	9.119	8.084	7.736	...	0.030	0.028	1	12	11	0.34	0YYY0Y
CHXR 30b	11 07 57.28	−77 17 26.4	13.278	11.119	9.825	0.204	0.150	0.096	12	12	11	3.46	Y0 0YYY
T29	11 07 57.91	−77 38 45.1	10.147	8.406	7.107	0.262	0.182	0.136	11	11	11	5.49	YY0 0YY
T30	11 07 58.07	−77 42 41.4	12.017	10.723	9.917	0.200	0.146	0.103	11	11	11	4.21	YY0 0Y0
CHXR 30a	11 07 59.98	−77 17 30.6	11.819	9.958	9.118	0.031	0.017	0.014	12	11	11	0.36	0 0 0YYY
T31	11 08 01.47	−77 42 28.9	8.692	7.640	6.947	0.083	0.083	0.090	18	15	17	2.60	YY0YYY
ISO 126	11 08 02.93	−77 38 42.8	11.574	9.636	8.205	0.095	0.093	0.070	16	18	20	2.36	Y0 0 0Y0
T32	11 08 03.26	−77 39 17.6	7.351	6.926	6.273	0.053	0.068	0.100	21	20	21	1.69	YY0YYY
T33	11 08 15.33	−77 33 53.5	8.356	7.189	6.182	0.119	0.114	0.089	19	25	25	2.85	YY0YYY
T34	11 08 16.46	−77 44 37.3	11.186	10.353	10.036	0.036	0.040	0.029	25	25	25	0.54	0Y0 0 0Y
Cha Ha 13	11 08 17.01	−77 44 12.0	11.792	11.045	10.660	0.037	0.035	0.022	25	25	25	0.37	0Y0 0 0 0
B40	11 08 17.9	−77 32 22	...	...	...	...	...	...	...	...	...	...	0 0 0 0 0Y
ISO 138	11 08 18.44	−77 30 41.0	14.054	13.464	13.051	0.046	0.039	0.048	25	25	25	−0.02	0Y0 0Y0
Cha Ha 4	11 08 18.93	−77 39 17.3	12.115	11.443	11.041	0.037	0.036	0.027	25	25	25	0.49	0Y0 0 0 0
ISO 143	11 08 22.33	−77 30 27.9	12.601	11.624	11.093	0.053	0.041	0.037	25	25	25	0.69	0Y0 0Y0
Cha Ha 10	11 08 24.02	−77 39 30.2	14.322	13.670	13.222	0.044	0.051	0.040	25	25	25	0.22	0Y0 0Y0
Cha Ha 5	11 08 24.08	−77 41 47.6	12.040	11.185	10.736	0.028	0.030	0.032	25	25	24	0.28	0Y0 0 0 0
ISO 145	11 08 25.77	−76 55 57.0	13.737	12.911	12.582	0.040	0.043	0.039	25	25	25	0.25	0 0 0 0Y0
ISO 147	11 08 26.45	−77 15 55.2	13.712	12.903	12.372	0.043	0.039	0.042	25	25	25	0.65	0 0 0 0Y0
Cha Ha 11	11 08 29.23	−77 39 19.9	14.598	13.947	13.507	0.067	0.050	0.054	25	25	25	0.27	0Y0 0 0 0
IRN	11 08 38.95	−77 43 51.4	...	...	...	...	...	...	...	...	...	...	0 0 0 0YY
T35	11 08 39.01	−77 16 04.2	11.265	9.931	9.045	0.320	0.200	0.120	25	25	24	6.31	YY0 0YY
Cha Ha 6	11 08 39.49	−77 34 16.8	12.270	11.497	11.026	0.032	0.030	0.026	25	25	25	0.28	0Y0 0Y0
CHXR 33	11 08 40.70	−76 36 07.9	10.587	9.650	9.295	0.029	0.032	0.023	25	25	24	0.34	0YYY0 0
ISO 154	11 08 43.05	−76 27 46.8	12.749	11.764	11.453	0.029	0.026	0.032	25	25	25	0.21	0 0 0 0Y0
T37	11 08 50.92	−76 25 13.7	12.404	11.729	11.332	0.027	0.037	0.028	24	25	23	0.19	0Y0 0Y0
T36	11 08 52.36	−76 43 59.6	13.535	12.993	12.809	0.165	0.123	0.113	24	25	24	3.19	Y0 0 0 0 0
CHXR 78C	11 08 54.19	−77 32 11.7	12.350	11.566	11.187	0.021	0.031	0.032	24	23	23	0.30	0Y0YYY
T38	11 08 54.61	−77 02 13.1	11.448	10.304	9.549	0.162	0.114	0.067	24	25	24	2.82	YY0 0Y0
ISO 164	11 08 54.75	−76 39 41.6	12.397	11.848	11.686	0.028	0.032	0.028	24	24	24	0.39	0 0 0 0Y0
ISO 165	11 08 54.98	−76 32 41.2	13.137	12.164	11.523	0.100	0.083	0.051	23	24	21	2.17	Y0 0 0Y0
Hn 7	11 09 05.10	−77 09 58.0	11.937	11.261	10.987	0.016	0.030	0.020	13	14	13	0.13	0Y0 0 0 0
ISO 177	11 09 07.92	−76 49 10.6	12.771	11.945	11.658	0.187	0.154	0.156	13	13	13	5.38	Y0 0 0Y0
T39	11 09 11.71	−77 29 12.6	...	...	...	...	...	...	...	...	...	...	0Y0Y0Y
CHXR 35	11 09 13.84	−76 28 39.6	11.849	11.185	10.894	0.027	0.035	0.022	13	13	13	0.16	0Y0Y0 0
OTS 7	11 09 16.5	−76 36 39	...	...	...	...	...	...	...	...	...	...	0 0 0 0Y0
CHXR 37	11 09 17.72	−76 27 57.8	10.017	9.041	8.700	0.018	0.029	0.021	13	13	13	−0.01	0YYY0 0
CHXR 79	11 09 18.15	−76 30 29.3	11.785	10.204	9.199	0.082	0.060	0.083	13	13	13	1.86	YY0YY 0
C 1-6	11 09 22.67	−76 34 32.1	12.737	10.392	8.769	0.259	0.185	0.149	13	13	13	4.53	Y0 0 0Y0
T40	11 09 23.80	−76 23 20.8	10.064	8.986	8.121	0.164	0.144	0.124	13	12	13	4.43	YY0YYY
OTS 11	11 09 24.1	−76 34 55	...	...	...	...	...	...	...	...	...	...	0 0 0 0Y0
Ced 112 IRS2	11 09 26.05	−76 33 33.8	13.258	11.251	10.237	0.031	0.025	0.026	13	13	13	0.17	0 0 0 0 0Y
ISO 192	11 09 28.55	−76 33 28.1	16.108	13.320	11.044	0.140	0.126	0.105	13	13	13	1.54	Y0 0 0Y0
CHXR 40	11 09 40.08	−76 28 39.2	10.096	9.209	8.955	0.023	0.028	0.028	14	16	16	0.13	0YYY0 0
C 1-25	11 09 41.91	−76 34 58.5	13.764	11.405	10.075	0.082	0.058	0.067	21	19	21	1.52	Y0 0 0Y0
C 7-1	11 09 42.55	−77 25 58.0	12.319	11.150	10.538	0.042	0.028	0.032	24	24	23	0.43	0 0 0 0YY
Hn 10W	11 09 43.07	−76 34 38.7	...	15.693	14.663	...	0.161	0.106	...	19	21	−0.14	0 0 0 0 0 0
C 2-3	11 09 45.86	−76 43 54.5	11.820	10.753	10.172	0.052	0.035	0.030	24	23	24	0.45	0 0 0 0 0 0

TABLE 5—*Continued*

Name (1)	α (J2000.0) (2)	δ (J2000.0) (3)	Mean Magnitudes[a] J (4)	H (5)	K_s (6)	rms[a] J (7)	H (8)	K_s (9)	N J (10)	H (11)	K_s (12)	Variability Index (13)	YSO Properties[b] (14)
Hn 10E	11 09 46.19	−76 34 46.5	11.993	10.755	10.114	0.052	0.039	0.035	24	23	23	0.65	0Y00YY
B43	11 09 47.37	−77 26 29.3	12.592	11.085	10.136	0.205	0.159	0.125	25	24	24	4.23	Y000YY
ISO 206	11 09 47.63	−76 51 18.2	16.503	14.468	13.480	0.139	0.076	0.070	25	25	25	0.17	00000Y0
ISO 209	11 09 48.62	−77 14 38.4	15.404	13.400	12.279	0.069	0.041	0.035	25	25	25	0.22	00000Y0
T41	11 09 50.01	−76 36 47.7	7.640	7.381	7.188	0.034	0.019	0.022	25	25	25	0.46	000YYY
ISO 216	11 09 51.98	−76 57 58.9	11.873	10.613	10.074	0.033	0.026	0.021	25	25	24	0.32	00000Y0
ISO 217	11 09 52.14	−76 39 12.8	13.538	12.512	11.767	0.050	0.040	0.037	25	25	24	0.51	00000Y0
ISO 220	11 09 53.31	−77 28 36.7	14.316	13.091	12.329	0.046	0.039	0.059	25	25	25	0.80	0Y00Y0
T42	11 09 53.40	−76 34 25.6	9.612	8.032	6.782	0.246	0.164	0.144	25	25	25	4.82	YY00YY
T43	11 09 54.06	−76 29 25.4	11.280	10.019	9.311	0.093	0.068	0.049	25	25	25	1.56	YY0YY0
ISO 225	11 09 54.38	−76 31 11.4	15.064	13.763	12.971	0.109	0.086	0.130	25	25	25	1.38	Y000Y0
C 1-2	11 09 55.05	−76 32 41.1	14.121	11.563	9.787	0.225	0.172	0.116	22	25	25	3.49	Y000YY
T45	11 09 58.68	−77 37 09.1	9.948	8.863	8.099	0.078	0.065	0.087	25	25	25	2.00	YY0YYY
T44	11 10 00.09	−76 34 57.9	8.777	7.319	6.180	0.073	0.063	0.043	25	25	25	1.35	YY0YY0
OTS 31	11 10 02.4	−76 32 37	...	...	...	...	...	...	...	...	...	...	00000Y0
OTS 32	11 10 03.35	−76 33 11.1	16.674	15.020	13.873	0.189	0.108	0.069	22	25	25	−0.08	00000Y0
Hn 11	11 10 03.69	−76 33 29.2	11.779	10.278	9.478	0.036	0.054	0.053	25	25	25	0.83	0Y00Y0
T45a	11 10 04.68	−76 35 45.2	10.530	9.609	9.221	0.069	0.069	0.060	25	25	25	1.86	Y00YYY
T46	11 10 07.04	−76 29 37.6	9.921	8.958	8.475	0.041	0.051	0.048	25	25	25	0.74	YY0YYY
ISO 235	11 10 07.83	−77 27 48.1	13.518	12.075	11.301	0.029	0.032	0.026	25	25	24	0.14	00000Y0
OTS 44	11 10 09.32	−76 32 18.0	16.365	15.317	14.602	0.157	0.163	0.093	24	25	25	−0.05	00000Y0
OTS 42	11 10 09.34	−76 35 06.4	15.413	14.035	13.393	0.063	0.045	0.064	25	25	25	0.04	00000Y0
ISO 237	11 10 11.40	−76 35 29.2	10.908	9.448	8.678	0.040	0.032	0.040	25	25	25	0.79	00000Y0
OTS 48	11 10 14.1	−76 34 37	...	...	...	...	...	...	...	...	...	...	00000Y0
Hn 12W	11 10 28.50	−77 16 59.6	11.716	11.059	10.728	0.028	0.031	0.030	25	25	23	0.13	0Y0000
OTS 56	11 10 30.0	−76 32 53	...	...	...	...	...	...	...	...	...	...	00000Y0
Hn 12E	11 10 30.67	−77 17 00.9	15.914	14.835	14.404	0.126	0.076	0.094	25	25	25	0.07	000000
OTS 59	11 10 32.0	−76 35 55	...	...	...	...	...	...	...	...	...	...	00000Y0
ISO 247	11 10 33.68	−76 39 22.4	13.245	11.947	11.347	0.028	0.034	0.032	16	17	14	0.27	00000Y0
ISO 250	11 10 36.42	−77 22 13.1	12.730	11.339	10.674	0.020	0.030	0.022	18	22	18	0.09	00000Y0
CHXR 47	11 10 38.00	−77 32 40.0	9.711	8.686	8.259	0.030	0.033	0.038	17	20	17	0.46	0YYYYY
ISO 252	11 10 41.40	−77 20 48.1	13.885	12.886	12.285	0.026	0.038	0.026	12	12	12	0.00	0Y00Y0
OTS 61	11 10 42.9	−76 34 05	...	...	...	...	...	...	...	...	...	...	00000Y0
T47	11 10 49.57	−77 17 51.8	11.398	10.094	9.311	0.095	0.071	0.070	12	12	12	1.68	YY00YY
T48	11 10 53.33	−76 34 32.0	11.214	10.445	9.956	0.046	0.037	0.051	12	12	12	1.11	YY0YY0
ISO 256	11 10 53.58	−77 25 00.6	13.999	12.242	11.156	0.398	0.312	0.219	12	11	12	8.11	YY00Y0
Hn 13	11 10 55.96	−76 45 32.6	11.244	10.419	9.919	0.049	0.048	0.029	12	12	12	0.85	0Y00Y0
B47	11 11 09.1	−77 26 19	...	...	...	...	...	...	...	...	...	...	00000Y
Hn 14	11 11 14.17	−76 41 11.1	14.128	12.996	12.612	0.049	0.045	0.038	13	13	13	0.27	0Y0000
ISO 274	11 11 25.48	−77 06 10.2	14.389	13.621	13.274	0.051	0.048	0.053	25	25	25	0.24	00000Y0
CHXR 48	11 11 34.74	−76 36 21.3	10.757	9.982	9.720	0.072	0.081	0.071	25	24	25	2.27	YYYY00
T49	11 11 39.67	−76 20 15.1	10.552	9.718	9.180	0.072	0.102	0.135	25	25	25	2.25	YY0 0YY
CHX 18N	11 11 46.34	−76 20 09.0	9.082	8.304	7.833	0.037	0.038	0.041	25	25	25	0.85	0YYY0Y
CHXR 49NE	11 11 54.01	−76 19 30.9	10.197	9.446	9.179	0.018	0.034	0.028	25	25	25	0.29	0YYY00
CHXR 84	11 12 03.28	−76 37 03.3	11.736	11.092	10.748	0.028	0.034	0.029	23	24	23	0.49	0Y0Y00
ISO 282	11 12 03.50	−77 26 00.9	13.286	12.323	11.682	0.314	0.226	0.152	25	25	22	6.73	Y000Y0
T50	11 12 09.84	−76 34 36.6	11.108	10.296	9.870	0.113	0.117	0.073	13	13	13	3.37	YY0Y00
T51	11 12 24.41	−76 37 06.5	9.201	8.431	8.021	0.041	0.021	0.026	13	13	13	−0.10	0Y0Y0Y
T52	11 12 27.71	−76 44 22.4	8.326	7.497	6.865	0.044	0.060	0.067	13	13	13	1.76	YY0YYY
CHXR 53	11 12 27.75	−76 25 29.3	10.887	10.208	9.980	0.022	0.025	0.030	13	13	13	0.28	0Y0Y00
T53	11 12 30.93	−76 44 24.1	10.975	9.878	9.209	0.234	0.154	0.106	13	13	13	4.16	YY00Y0
CHXR 54	11 12 42.10	−76 58 40.1	10.422	9.699	9.500	0.034	0.045	0.036	13	13	11	0.74	0YYY00
T54	11 12 42.67	−77 22 23.0	8.625	8.033	7.861	0.020	0.027	0.018	14	14	14	0.16	0Y0Y0Y
CHXR 55	11 12 42.98	−76 37 05.0	10.039	9.397	9.251	0.025	0.034	0.039	13	13	13	0.70	0YYY00
Hn 17	11 12 48.59	−76 47 06.7	12.087	11.425	11.151	0.039	0.037	0.045	20	19	20	0.89	0Y0000
CHXR 57	11 13 20.13	−77 01 04.4	10.938	10.220	9.985	0.035	0.034	0.026	25	24	24	0.53	0YYY0Y
Hn 18	11 13 24.45	−76 29 22.9	11.848	11.106	10.764	0.024	0.033	0.047	25	25	23	0.22	0Y0000
CHXR 59	11 13 27.36	−76 34 16.7	10.584	9.853	9.621	0.030	0.035	0.033	25	25	25	0.53	0YYY00
CHXR 60	11 13 29.69	−76 29 01.4	11.554	10.839	10.552	0.023	0.028	0.027	25	25	24	0.10	0Y0Y00
IRAS 11120−7750	11 13 30.32	−78 07 02.4	6.804	5.783	5.346	0.035	0.028	0.028	25	25	25	0.98	00000Y
T55	11 13 33.56	−76 35 37.5	11.638	11.012	10.727	0.044	0.054	0.048	25	25	25	0.83	YY0Y00
CHXR 62	11 14 15.64	−76 27 36.6	11.257	10.443	10.122	0.024	0.024	0.027	12	12	12	0.23	0Y0Y00
Hn 21W	11 14 24.50	−77 33 06.4	11.986	11.049	10.597	0.043	0.036	0.038	24	24	25	0.20	0Y0000

TABLE 5—*Continued*

Name (1)	α (J2000.0) (2)	δ (J2000.0) (3)	Mean Magnitudes[a] J (4)	H (5)	K_s (6)	rms[a] J (7)	H (8)	K_s (9)	N J (10)	H (11)	K_s (12)	Variability Index (13)	YSO Properties[b] (14)
Hn 21E	11 14 26.09	−77 33 04.4	12.754	11.941	11.484	0.036	0.035	0.038	25	25	25	0.20	0 0 0 0 0 0
B53	11 14 50.30	−77 33 38.8	10.463	9.742	9.496	0.021	0.026	0.027	25	25	25	0.10	0 0 0 0 0 Y
CHXR 65B	11 16 11.95	−77 14 10.1	14.170	13.619	13.357	0.056	0.027	0.052	12	13	13	0.18	0 0 0 Y 0 0
CHXR 65A	11 16 12.91	−77 14 06.5	11.061	10.464	10.312	0.039	0.024	0.038	14	14	13	0.28	0 Y 0 Y 0 Y
T56	11 17 36.95	−77 04 38.0	10.293	9.562	9.267	0.024	0.027	0.028	1	1	1	...	0 Y 0 Y 0 Y
CHXR 68B	11 18 19.54	−76 22 01.4	11.264	10.539	10.297	0.028	0.026	0.029	1	1	1	...	0 0 0 Y 0 0
CHXR 68A	11 18 20.21	−76 21 57.7	9.772	9.063	8.829	0.026	0.027	0.030	1	1	1	...	0 YYY 0 0
IRAS 11248−7653	11 26 41.5	−77 10 15	...	...	...	...	...	...	...	...	...	...	0 0 0 0 0 Y

[a] For sources with J, H, and K_s photometry, $N = 1$ in all three bands, but otherwise no tabulated Stetson index, the photometry is from the Version 2 processing of the 2MASS Working Database, and the rms represents the photometric uncertainty from the 2MASS processing pipeline.

[b] Six character flag indicating the properties of that star. References provided in the text. First character: variable identified from this study or General Catalog of Variable Stars. Second character: contains Hα in emission. Third character: contains lithium in absorption. Fourth character: X-ray source. Fifth character: contains an infrared excess. Sixth character: far-infrared source.

from left to right, (1) known variables from the General Catalog of Variable Stars or this study; (2) Hα-emitting objects from Henize & Mendoza (1973), Schwartz (1977), Hartigan (1993), Walter (1992), Huenemoerder et al. (1994), Lawson et al. (1996), Comerón et al. (1999), and Comerón et al. (2000), and objects with Paβ or Brγ in emission from Gómez & Persi (2002); (3) stars with lithium in absorption from Walter (1992), Huenemoerder et al. (1994), and Lawson et al. (1996); (4) X-ray sources from Feigelson & Kriss (1989) and Feigelson et al. (1993); (5) near- or mid-infrared excesses from Oasa et al. (1999), Persi et al. (2000), and this study; and (6) far-infrared sources from Baud et al. (1984), Assendorp et al. (1990), Prusti et al. (1991), and the *IRAS* Point Source Catalog. The flag "Y" indicates the characteristic has been identified with that star in at least one study; The flag "?" indicates that the authors of the original paper expressed uncertainty of the detection; and the flag "0" indicates the property has not yet been identified.

Notes on individual sources:

UX Cha.—Feigelson & Kriss (1989) associated UX Cha (=T22) with the X-ray source CHX 8. However, as originally noted by Feigelson et al. (1993), UX Cha is actually located 26″ to the north. The finder chart in Schwartz (1991) identifies the incorrect star as UX Cha.

C9-1, C9-2, and C9-3.—Hyland et al. (1982) identified these objects as Chamaeleon I members based on bolometer data. Each of these objects is located in the bright Infrared Nebula (IRN). However, none of these sources are visible on the 2MASS images. While it is possible that these objects are variable and have faded from view, we find it more likely that they are knots in nebulosity and have not included these objects in the membership list.

T2.—This source has been traditionally identified as a member of Chamaeleon I based on its optical variability. However, Winterberg & Bruch (1996) showed that this source is a RR Lyrae star unrelated to Chamaeleon I. This source is not listed in Table 5.

T36.—This source has traditionally been associated with Chamaeleon I based on its optical variability, but the near-infrared colors and magnitudes of this star ($K_s = 12.809$, $H-K_s = 0.184$) are inconsistent with membership. While this star is listed in Table 5, spectroscopic observations are needed to ascertain membership.

T49, CHX 18N, and IRAS 11101−7603.—The *IRAS* source is closest to CHX 18N, but within the *IRAS* astrometric uncertainties may also be associated with T49. It is listed under both objects in Table 5.

T52 and T53.—Feigelson & Kriss (1989) lists both sources as possible optical counterparts to the X-ray source CHX 19. Subsequent high-resolution observations with *ROSAT* show the X-ray emission originates from T52 (Feigelson et al. 1993). Therefore, we have not listed T53 as a counterpart to CHX 19 in Table 6.

CHXR 30 and B38.—Lawson et al. (1996) associates CHXR 30 with B38, while Cambrésy et al. (1998) and Kenyon & Gómez (2001) list CHXR 30 and B38 as separate sources. Two stars separated by 9.″9 are present on the 2MASS images. The eastern source is consistently identified as CHXR 30 in these studies. It is the brighter of the two 2MASS sources in the optical with a $J-K_s$ color of 2.70. This star has not been conclusively identified as a pre–main-sequence object through spectroscopy, although Persi et al. (2000) identified a mid-infrared excess in this source from *ISO* observations. The western source, identified as B38 (Baud et al. 1984) by Cambrésy et al. (1998) and Kenyon & Gómez (2001), is the redder of the two 2MASS objects with $J-K_s = 3.45$. This source is detected as a variable with a near-infrared excess in our observations. Since the resolution of the *IRAS* observations used by Baud et al. (1984) encompasses both 2MASS sources and the position uncertainty of the *ROSAT* X-ray observations is 8″, it is not clear which, or whether both, sources contribute to the far-infrared and X-ray emission. In Table 5, we list the eastern source as CHXR 30a and B38a, and the western source as CHXR 30b and B38b.

HM 8 and ISO 10.—Persi et al. (2000) tentatively matched ISO 10 with HM 8, but they noted larger than average positional differences between the two objects. The positional difference is larger than the tolerance limit used here to match the *ISO* catalog with the 2MASS astrometry, and this association was not made in Table 5.

TABLE 6

CROSS IDENTIFICATION OF CHAMAELEON I MEMBERS

Name	CHSM	Cam98	GCVS	W87	Sz77	Hoff63	HM73	F93	FK89	Hn93	H82/J85	HBC88	P00	KG01	GK01	OTS99	B84	IRAS	Other
T1	...	Cam1 1	...	T1	Sz 1	...	...	...	...	...	...	...	...	...	...	...	...	...	...
IRAS 10529−7638	...	...	...	...	...	...	...	...	...	...	...	...	...	...	...	...	...	10529−7638	...
T2	...	Cam1 2	SW Cha	T2	...	S6319	...	...	...	...	...	...	...	...	...	...	...	...	...
T3	...	Cam1 3	SX Cha	T3	Sz 2	S6320	HM 1	...	...	...	...	HBC 564	...	...	...	...	B1	10548−7708	...
T4	...	Cam1 4	SY Cha	T4	Sz 3	S6321	HM 2	CHXR 1	CHX 1	...	...	HBC 565	...	...	...	...	B2	10552−7655	...
T5	...	Cam1 5	...	T5	Sz 4	...	...	...	...	...	...	...	...	...	...	...	...	...	...
CHXR 3	...	Cam1 6	...	...	...	...	...	CHXR 3	...	...	...	...	...	...	...	...	B3	...	...
T6	...	Cam1 7	SZ Cha	T6	...	S6323	...	CHXR 4	CHX 2	...	...	HBC 566	...	...	...	...	B4	10570−7701	Glass V
T7	...	Cam1 8	TW Cha	T7	Sz 5	S6326	HM 3	CHXR 5	...	...	...	HBC 567	...	...	...	...	B5	10577−7706	...
T8	...	Cam1 9	CR Cha	T8	Sz 6	...	HM 4	CHXR 6	CHX 3	...	...	HBC 244	...	...	...	...	B6	10578−7645	LkHa 332-20
T9	...	Cam1 10	...	T9	Sz 7	...	HM 5	...	...	...	...	...	...	...	...	...	...	10589−7628	...
CHXR 8	...	Cam1 11	...	...	...	...	...	CHXR 8	...	...	...	...	...	...	...	...	B8	...	...
T10	...	Cam1 12	...	T10	Sz 8	...	HM 6	...	...	...	...	...	...	...	...	...	...	...	...
CHXR 9C	...	Cam1 13	...	...	...	...	...	CHXR 9C	...	...	...	...	...	...	...	...	...	...	...
B23	...	...	...	...	...	...	...	...	...	...	...	...	...	...	...	...	B23	...	...
B9	...	Cam1 14	...	...	...	...	...	...	...	...	...	...	...	...	...	...	B9	...	...
ISO 1	...	...	...	...	...	...	...	...	...	...	...	...	ISO 1	...	...	...	...	...	...
T11	...	Cam1 15	CS Cha	T11	Sz 9	...	HM 7	CHXR 10	CHX 4	...	...	HBC 569	ISO 3	...	...	...	B10	11011−7717	...
CHXR 71	...	Cam1 16	...	...	...	...	...	CHXR 71	...	Hn 1	...	...	ISO 4	...	...	...	B11	...	...
ISO 13	...	...	...	...	...	...	...	...	...	...	...	...	ISO 13	...	...	...	...	...	...
T12	...	Cam1 17	...	T12	Sz 10	...	HM 8	...	...	...	...	...	...	...	...	...	...	...	...
CHXR 11	...	Cam1 18	...	...	...	...	...	CHXR 11	...	...	...	...	ISO 17	...	...	...	B12	...	...
ISO 28	757	...	...	...	...	...	...	...	...	...	...	...	ISO 28	...	...	...	...	...	...
Hn 2	1012	Cam1 19	...	...	...	...	...	...	...	Hn 2	...	...	ISO 32	...	...	...	B13a	...	...
T13	1154	Cam1 20	TZ Cha	T13	...	S6334	...	...	...	...	...	...	...	...	...	...	...	...	...
CHXR 12	1403	Cam1 21	...	...	...	...	...	CHXR 12	...	Hn 3	...	...	ISO 34	...	...	...	B14	...	...
T14	1898	Cam1 22	CT Cha	T14	Sz 11	...	HM 9	CHXR 13	...	...	...	HBC 570	...	...	...	...	...	11027−7611	...
CHXR 72	2002	Cam1 23	...	...	...	...	...	CHXR 72	...	...	...	...	...	...	...	...	...	...	...
T14a	2482	Cam1 24	...	T14a	...	...	...	...	...	...	...	...	ISO 46	...	...	...	...	11030−7702	HH 48
T15	2553	Cam1 25	...	T15	Sz 12	...	HM 10	...	...	...	...	...	ISO 48	...	...	...	...	...	...
ISO 52	3319	Cam1 26	...	...	...	...	...	...	...	...	...	...	ISO 52	...	...	...	B18	...	...
CHXR 14N	3657	Cam1 27	...	...	...	...	...	CHXR 14N	...	...	...	...	...	...	...	...	...	...	...
CHXR 14S	3716	Cam1 28	...	...	...	...	...	CHXR 14S	...	...	...	...	...	...	...	...	...	...	...
T16	3876	Cam1 29	...	T16	Sz 13	...	...	...	...	...	...	...	ISO 55	...	...	...	B19	...	...
B29	...	...	...	...	...	...	...	...	...	...	...	...	...	...	...	...	B29	...	...
Hn 4	4629	Cam1 30	...	...	...	...	...	...	...	Hn 4	...	...	...	...	...	...	...	...	...
T18	4649	Cam1 31	...	T18	Sz 14	...	...	...	...	...	...	...	...	...	...	...	...	...	...
T17	4943	Cam1 32	UU Cha	T17	...	S6335	...	...	...	...	...	...	...	...	...	...	...	...	...
T19	5797	Cam1 33	...	T19	Sz 15	...	...	...	...	...	...	...	...	...	...	...	...	...	...
CHXR 15	5856	Cam1 34	...	...	...	...	...	CHXR 15	...	...	...	...	ISO 65	...	...	...	B22	...	...
T20	6267	Cam1 35	UV Cha	T20	...	S6336	...	CHXR 18	...	...	...	HBC 571	...	...	...	...	...	...	...
ISO 68	6314	...	...	...	...	...	...	...	...	...	...	...	ISO 68	...	...	...	...	...	...
ISO 71	6738	...	...	...	...	...	...	...	...	...	...	...	ISO 71	...	...	...	...	...	...
T21	7184	Cam1 36	...	T21	...	...	...	CHXR 19	CHX 7	...	...	...	ISO 75	...	...	...	...	11048−7706	Glass F, Ced 110, Ced 110 IRS 2
B31	...	...	...	...	...	...	...	...	...	...	...	...	...	...	...	...	B31	...	...
CHXR 73	7730	...	...	...	...	...	...	CHXR 73	...	...	...	...	ISO 78	...	...	...	B25	...	...
Cha Ha 12	8077	...	...	...	...	...	...	...	...	...	...	...	...	...	...	...	...	...	...
ISO 79	8134	...	...	...	...	...	...	...	...	...	...	...	ISO 79	...	GK 13	...	...	...	...
Hn 5	8234	Cam1 37	...	...	...	...	...	...	...	Hn 5	...	...	...	...	...	...	...	...	...
T22	8284	Cam1 38	UX Cha	T22	...	S6337	...	...	...	...	...	...	ISO 80	...	...	...	...	...	...
CHXR 20	8369	Cam1 39	...	...	...	...	...	CHXR 20	CHX 8	...	...	...	ISO 81	...	...	...	B26	...	Ced 110 IRS 3

TABLE 6—*Continued*

Name	CHSM	Cam98	GCVS	W87	Sz77	Hoff63	HM73	F93	FK89	Hn93	H82/J85	HBC88	P00	KG01	GK01	OTS99	B84	IRAS	Other
Ced 110 IRS4	8415	Cam1 40	...	...	...	...	...	...	...	...	...	...	ISO 84	...	...	...	...	11051−7706	Ced 110 IRS 4
CHXR 74	8892	...	...	...	...	...	...	CHXR 74	...	...	...	...	ISO 87	...	...	...	B27	...	...
ISO 86	8924	...	...	...	...	...	...	...	...	...	...	...	ISO 86	...	...	...	...	...	...
T23	8978	Cam1 41	UY Cha	T23	Sz 16	S6340	HM 11	...	...	...	...	...	ISO 89	...	...	...	...	...	Ced 110 IRS 5
Ced 110 IRS6	9387	Cam1 42	...	...	...	...	...	...	...	...	...	...	ISO 92	...	...	...	...	11057−7706	Ced 110 IRS 6
ISO 91	9391	Cam2 21	...	...	...	...	...	...	...	...	...	...	ISO 91	...	...	...	...	...	...
CHXR 22W	9433	Cam1 43	...	...	...	...	...	CHXR 22W	...	...	...	...	ISO 93	...	...	...	...	...	...
CHXR 21	9467	Cam1 44	...	...	...	...	...	CHXR 21	...	Hn 6	...	...	ISO 94	KG 1	...	...	B28	...	...
T24	9496	Cam1 45	UZ Cha	T24	Sz 17	S6341	...	CHXR 75	...	...	...	...	...	...	...	...	...	...	...
CHXR 22E	9542	Cam1 46	...	...	...	...	...	CHXR 22E	...	...	...	...	...	KG 2	...	...	B29	...	...
ISO 97	9652	Cam2 23	...	...	...	...	...	...	...	...	...	...	ISO 97	KG 3	...	...	...	...	...
Cha Ha 1	9671	...	...	...	...	...	...	...	...	...	...	...	ISO 95	...	...	...	...	...	...
Cha Ha 9	9753	...	...	...	...	...	...	...	...	...	...	...	ISO 98	...	...	...	...	...	...
T25	9782	Cam1 47	...	T25	Sz 18	...	HM 12	...	...	...	...	HBC 572	...	...	...	...	...	11057−7546	...
T26	9847	Cam1 48	DI Cha	T26	Sz 19	...	HM 13	CHXR 23	CHX 9	...	...	HBC 245	ISO 100	KG 6	...	...	B32	11059−7721	LkHa 332-17, Ced 111 IRS 1
B35	9872	Cam2 24	...	...	...	...	...	...	...	...	...	...	ISO 101	KG 7	...	...	B35	...	...
T27	10138	Cam1 49	VV Cha	T27	Sz 20	S6342	HM 14	CHXR 24	...	...	...	HBC 573	...	KG 12	...	...	...	...	...
CHXR 25	10307	Cam1 50	...	...	...	...	...	CHXR 25	...	...	...	...	ISO 105	KG 13	...	...	B33	...	...
CHXR 76	10394	Cam1 51	...	...	...	...	...	CHXR 76	...	...	...	...	ISO 106	KG 15	...	...	B34	...	...
CHXR 26	10464	Cam1 52	...	...	...	...	...	CHXR 26	...	...	...	...	ISO 108	KG 17	...	...	B35	...	...
Cha Ha 7	10496	Cam2 26	...	...	...	...	...	...	...	...	...	...	...	...	...	...	...	...	...
Cha Ha 2	10685	...	...	...	...	...	...	...	...	...	...	...	ISO 111	KG 20	...	...	...	...	...
T28	10737	Cam1 53	...	T28	Sz 21	...	HM 15	CHXR 27	...	...	...	HBC 574	ISO 112	KG 21	...	...	B36	...	...
Cha Ha 8	10837	...	...	...	...	...	...	...	...	...	...	...	...	...	...	...	...	...	...
ISO 114	11070	...	...	...	...	...	...	...	...	...	...	...	ISO 114	...	...	...	...	...	...
Cha Ha 3	11114	...	...	...	...	...	...	...	...	...	...	...	ISO 116	KG 23	...	...	...	...	...
CHXR 28	11256	Cam1 54	...	...	...	...	...	CHXR 28	CHX 10a	...	...	...	ISO 117	KG 24	...	...	B37	...	...
CHXR 30b	11315	Cam1 55	...	...	...	...	...	CHXR 30b	...	...	...	...	...	KG 26	...	...	B38b	11065−7701	Ced 110 IRS 7
T29	11344	Cam1 56	...	T29	Sz 22	...	HM 16	...	...	...	...	...	ISO 119	KG 28	...	...	B39	...	...
T30	11351	Cam1 57	...	T30	Sz 23	...	...	...	...	...	...	...	ISO 120	KG 27	...	...	...	...	...
CHXR 30a	11416	Cam1 58	...	...	...	...	...	CHXR 30a	...	...	...	...	ISO 122	KG 30	...	...	B38a	...	...
T31	11462	Cam1 59	VW Cha	T31	Sz 24	S6343	HM 17	CHXR 31	CHX 11	...	...	HBC 575	ISO 123	KG 31	...	...	B40	...	Ced 111 IRS 3
ISO 126	11529	Cam2 32	...	...	...	...	...	...	...	...	...	...	ISO 126	KG 33	...	...	...	...	...
T32	11547	Cam1 60	CU Cha	T32	Sz 25	...	HM 18	CHXR 29	...	...	...	HBC 246	ISO 124	KG 34	...	...	...	11066−7722	HD 97048, Ced 111 IRS 2
T33	12055	Cam1 61	...	T33	...	...	...	CHXR 32	CHX 12	...	...	...	ISO 135	KG 39	...	...	B42	11068−7717	Glass I, Ced 111 IRS 4
T34	12090	Cam1 62	...	T34	Sz 26	...	HM 19	...	...	...	...	...	ISO 136	KG 40	...	...	B44	...	...
Cha Ha 13	12108	...	...	...	...	...	...	...	...	...	...	...	ISO 137	KG 41	...	...	...	...	...
B40	...	...	...	...	...	...	...	...	...	...	...	...	...	...	...	...	B40	...	...
ISO 138	12159	...	...	...	...	...	...	...	...	...	...	...	ISO 138	...	...	...	...	...	...
Cha Ha 4	12180	...	...	...	...	...	...	...	...	...	...	...	...	...	...	...	...	...	...
ISO 143	12355	...	...	...	...	...	...	...	...	...	...	...	ISO 143	KG 45	...	...	c...	...	...
Cha Ha 10	12438	...	...	...	...	...	...	...	...	...	...	...	...	...	...	...	...	...	...
Cha Ha 5	12442	...	...	...	...	...	...	...	...	...	...	...	ISO 144	KG 47	...	...	...	...	...
ISO 145	12496	...	...	...	...	...	...	...	...	...	...	...	ISO 145	...	...	...	...	...	...
ISO 147	12525	...	...	...	...	...	...	...	...	...	...	...	ISO 147	...	...	...	...	...	...
Cha Ha 11	12653	...	...	...	...	...	...	...	...	...	...	...	...	...	...	...	...	...	...
IRN	13053	Cam1 63	...	...	...	...	...	...	...	...	...	...	ISO 150	KG 49	...	...	...	11072−7727	Ced 111 IRS 5
T35	13058	Cam1 64	...	T35	Sz 27	...	HM 20	...	...	...	C6-1	HBC 576	ISO 151	KG 50	...	...	...	...	Ced 110 IRS 8
Cha Ha 6	13082	...	...	...	...	...	...	...	...	...	...	...	ISO 152	KG 51	...	...	...	...	...
CHXR 33	13131	Cam1 65	...	...	...	...	...	CHXR 33	CHX 13a	...	C1-10	...	ISO 153	KG 52	...	...	...	...	...

TABLE 6—*Continued*

Name	CHSM	Cam98	GCVS	W87	Sz77	Hoff63	HM73	F93	FK89	Hn93	H82/J85	HBC88	P00	KG01	GK01	OTS99	B84	IRAS	Other
ISO 154	13217	...	...	...	...	...	...	...	...	...	...	...	ISO 154	...	...	...	...	...	...
T37	13553	Cam1 68	...	T37	Sz 28	...	...	...	...	...	...	...	ISO 157	KG 54	...	...	...	...	...
T36	13616	Cam1 66	VX Cha	T36	...	S6345	...	...	...	...	...	...	...	...	...	...	...	...	...
CHXR 78C	13696	Cam1 69	...	...	...	...	...	CHXR 78C	...	...	...	...	ISO 160	KG 56	...	...	B45	...	...
T38	13707	Cam1 70	VY Cha	T38	Sz 29	S6346	HM 21	...	...	...	C4-5	HBC 577	ISO 162	KG 58	...	...	...	...	...
ISO 164	13713	...	...	...	...	...	...	...	...	...	...	...	ISO 164	...	...	...	...	...	...
ISO 165	13720	...	...	...	...	...	...	...	...	...	...	...	ISO 165	KG 59	...	...	...	...	...
Hn 7	14124	Cam1 71	...	...	...	...	...	...	...	Hn 7	...	...	ISO 174	...	...	...	...	...	...
ISO 177	14235	...	...	...	...	...	...	...	...	...	...	...	ISO 177	KG 71	...	...	...	...	...
T39	14388	Cam1 72	...	T39	Sz 30	...	...	CHXR 36	CHX 14	...	C7-7	...	ISO 182	KG 74	...	...	B46	...	...
CHXR 35	14469	Cam1 73	...	...	...	...	...	CHXR 35	...	Hn 8	C1-15	...	...	KG 75	...	...	...	...	...
OTS 7	...	...	...	...	...	...	...	...	...	...	...	...	...	...	...	OTS 7	...	...	...
CHXR 37	14604	Cam1 74	...	...	...	...	...	CHXR 37	...	...	...	...	ISO 185	KG 77	...	...	...	...	...
CHXR 79	14623	Cam1 75	...	...	...	...	...	CHXR 79	...	Hn 9	C1-18	...	ISO 186	KG 79	...	...	...	...	...
C 1-6	14800	Cam1 76	...	...	...	...	...	...	...	...	C1-6	...	ISO 189	KG 82	...	OTS 10	...	...	...
T40	14843	Cam1 77	VZ Cha	T40	Sz 31	S6347	HM 22	CHXR 39	...	...	...	HBC 578	...	KG 83	...	...	...	11078−7607	Ced 112 IRS 1
OTS 11	...	...	...	...	...	...	...	...	...	...	...	...	...	...	GK 82	OTS 11	...	...	...
Ced 112 IRS2	14947	Cam2 40	...	...	...	...	...	...	...	...	C1-3	...	...	KG 85	...	OTS 13	...	...	Ced 112 IRS 2
ISO 192	15044	Cam2 41	...	...	...	...	...	...	...	...	...	...	ISO 192	KG 87	...	OTS 15	...	...	...
CHXR 40	15504	Cam1 78	...	...	...	...	...	CHXR 40	CHX 15b	...	...	...	ISO 198	KG 92	...	...	...	...	...
C 1-25	15576	Cam1 79	...	...	...	...	...	...	...	...	C1-25	...	ISO 199	KG 93	...	OTS 19	...	...	...
C 7-1	15600	Cam1 80	...	...	...	...	...	...	...	...	C7-1	...	ISO 200	KG 95	...	...	...	...	Ced 110 IRS 9
Hn 10W	15622	Cam1 83	...	...	...	...	...	...	...	Hn 10W	...	...	...	...	...	OTS 20	...	...	...
C 2-3	15732	Cam1 81	...	...	...	...	...	...	...	...	C2-3	...	ISO 203	KG 99	...	...	...	...	...
Hn 10E	15745	Cam1 82	...	T42	Sz 32	...	HM 23	...	...	Hn 10E	C1-24	...	ISO 204	KG 97	...	OTS 24	...	11083−7618	Ced 112 IRS 4
B43	15784	Cam1 84	...	...	...	...	...	...	...	...	...	...	ISO 207	KG 101	...	...	B43	...	...
ISO 206	15796	...	...	...	...	...	...	...	...	...	...	...	ISO 206	...	...	...	...	...	...
ISO 209	15850	Cam2 45	...	...	...	...	...	...	...	...	...	...	ISO 209	...	...	...	...	...	...
T41	15900	Cam1 85	...	T41	...	...	...	CHXR 42	...	...	C1-11	...	ISO 211	KG 103	...	OTS 26	...	11082−7620	HD 97300, Ced 112 IRS 3
ISO 216	15973	...	...	...	...	...	...	...	...	...	C4-1	...	ISO 216	KG 107	...	...	...	...	...
ISO 217	15980	...	...	...	...	...	...	...	...	...	...	...	ISO 217	KG 106	GK 29	...	...	...	...
ISO 220	16023	...	...	...	...	...	...	...	...	...	...	...	ISO 220	...	GK 30	...	...	...	...
T42	16026	Cam1 86	...	T42	Sz 32	...	HM 23	...	...	...	C1-5	HBC 579	ISO 223	KG 109	...	OTS 27	...	11083−7618	...
T43	16052	Cam1 87	...	T43	Sz 33	...	...	CHXR 41	CHX 15	...	C1-17	...	ISO 224	KG 110	...	...	...	...	...
ISO 225	16067	...	...	...	...	...	...	...	...	...	...	...	ISO 225	...	GK 31	...	...	...	...
C 1-2	16096	Cam1 88	...	...	...	...	...	...	...	...	C1-2	...	ISO 226	KG 111	...	OTS 28	...	...	Ced 112 IRS 5
T45	16254	Cam1 89	WX Cha	T45	Sz 35	S6349	HM 25	CHXR 43	CHX 17	...	C8-3	HBC 581	ISO 228	KG 114	...	...	B48	11085−7720	Ced 111 IRS 6
T44	16307	Cam1 90	WW Cha	T44	Sz 34	S6348	HM 24	CHXR 44	...	...	C1-7	HBC 580	ISO 231	KG 116	...	OTS 29	...	...	...
OTS 31	...	...	...	...	...	...	...	...	...	...	...	...	...	...	...	OTS 31	...	...	...
OTS 32	16422	...	...	...	...	...	...	...	...	...	...	...	...	...	...	OTS 32	...	...	...
Hn 11	16436	Cam1 91	...	...	...	...	...	...	...	Hn 11	C1-4	...	ISO 232	KG 117	...	OTS 33	...	...	...
T45a	16470	Cam1 92	...	T45a	...	...	...	CHXR 45	CHX 16	...	C1-9	HBC 582	ISO 233	KG 118	...	OTS 35	...	...	GK-1
T46	16560	Cam1 93	WY Cha	T46	Sz 36	S6351	HM 26	CHXR 46	...	...	C1-16	HBC 583	ISO 234	KG 119	...	...	...	11085−7613	Ced 112 IRS 6
ISO 235	16611	...	...	...	...	...	...	...	...	...	...	...	ISO 235	KG 120	...	...	...	...	...
OTS 44	16658	...	...	...	...	...	...	...	...	...	...	...	...	...	...	OTS 44	...	...	...
OTS 42	16659	...	...	...	...	...	...	...	...	...	...	...	...	...	...	OTS 42	...	...	...
ISO 237	16751	Cam2 48	...	...	...	...	...	...	...	...	C1-8	...	ISO 237	KG 121	...	OTS 45	...	...	...
OTS 48	...	...	...	...	...	...	...	...	...	...	...	...	...	...	...	OTS 48	...	...	...
Hn 12W	17417	Cam1 94	...	...	...	...	...	...	...	Hn 12W	C6-2	...	ISO 244	...	...	...	...	...	...
OTS 56	...	...	...	...	...	...	...	...	...	...	...	...	...	...	...	OTS 56	...	...	...
Hn 12E	17515	Cam1 95	...	...	...	...	...	...	...	Hn 12E	...	...	...	...	...	...	...	...	...
OTS 59	...	...	...	...	...	...	...	...	...	...	...	...	...	...	...	OTS 59	...	...	...
ISO 247	17625	...	...	...	...	...	...	...	...	...	...	...	ISO 247	...	...	...	...	...	...

TABLE 6—*Continued*

Name	CHSM	Cam98	GCVS	W87	Sz77	Hoff63	HM73	F93	FK89	Hn93	H82/J85	HBC88	P00	KG01	GK01	OTS99	B84	IRAS	Other
ISO 250	17743	...	...	...	...	...	...	...	...	...	...	...	ISO 250	...	...	...	...	...	...
CHXR 47	17807	Cam1 96	...	F 34	...	...	...	CHXR 47	...	...	C7-11	...	ISO 251	KG 124	...	...	B50	11091−7716	Glass Q, Ced 111 IRS 7
ISO 252	17959	...	...	...	...	...	...	...	...	...	...	...	ISO 252	...	...	...	...	...	...
OTS 61	...	...	...	...	...	...	...	...	...	...	...	...	...	...	...	OTS 61	...	...	...
T47	18261	Cam1 97	...	T47	Sz 37	...	HM 27	...	...	...	...	HBC 584	ISO 254	...	...	...	...	11093−7701	...
T48	18403	Cam1 98	WZ Cha	T48	Sz 38	S6352	HM 28	CHXR 82	...	...	C1-23	HBC 585	ISO 258	...	...	...	...	...	...
ISO 256	18416	Cam2 49	...	...	...	...	...	...	...	...	...	...	ISO 256	...	...	...	...	...	...
Hn 13	18502	Cam1 99	...	...	...	...	...	...	...	Hn 13	C2-5	...	ISO 259	...	...	...	...	...	...
B47	...	...	...	...	...	...	...	...	...	...	...	...	...	...	...	...	B47	...	...
Hn 14	19316	Cam1 100	...	...	...	...	...	...	...	Hn 14	...	...	...	...	...	...	...	...	...
ISO 274	19793	...	...	...	...	...	...	...	...	...	...	...	ISO 274	...	...	...	...	...	...
CHXR 48	20217	Cam1 101	...	...	...	...	...	CHXR 48	...	...	E1-7	...	ISO 280	...	...	...	...	...	...
T49	20409	Cam1 102	XX Cha	T49	Sz 39	...	HM 29	...	...	...	...	HBC 586	...	...	...	...	...	11101−7603	...
CHX 18N	20702	Cam1 103	...	...	...	...	...	...	CHX 18N	...	...	...	...	...	...	...	...	11101−7603	...
CHXR 49NE	21078	Cam1 104	...	...	...	...	...	CHXR 49NE	CHX 18	Hn 15	...	...	...	...	...	...	...	...	...
CHXR 84	21466	Cam1 105	...	...	...	...	...	CHXR 84	...	Hn 16	E1-10	...	...	...	...	...	...	...	...
ISO 282	21473	...	...	...	...	...	...	...	...	...	...	...	ISO 282	...	...	...	...	...	...
T50	21745	Cam1 106	...	T50	Sz 40	...	...	CHXR 85	...	...	E1-5	HBC 587	...	...	...	...	...	...	...
T51	22361	Cam1 107	...	T51	Sz 41	...	...	CHXR 50	CHX 20b	...	E1-9a	HBC 588	...	...	...	...	...	11108−7620	Ced 112 IRS 7
T52	22521	Cam1 108	CV Cha	T52	Sz 42	...	HM 30	CHXR 51	CHX 19	...	E2-4	HBC 247	...	...	...	...	...	11108−7627	LkHa 332-21, Ced 112 IRS 8
CHXR 53	22524	Cam1 109	...	...	...	...	...	CHXR 53	...	...	...	...	...	...	...	...	...	...	...
T53	22662	Cam1 110	CW Cha	T53	Sz 43	...	HM 31	...	...	...	...	HBC 589	...	...	...	...	...	...	...
CHXR 54	23146	Cam1 111	...	...	...	...	...	CHXR 54	CHX 21a	...	E4-3	...	...	...	...	...	...	...	...
T54	23172	Cam1 112	...	T54	...	...	HM Anon	CHXR 56	CHX 22	...	...	...	...	...	...	...	B51	11111−7705	...
CHXR 55	23183	Cam1 113	...	...	...	...	...	CHXR 55	CHX 20E	...	E1-8	...	...	...	...	...	...	...	...
Hn 17	23447	Cam1 114	...	...	...	...	...	...	...	Hn 17	E2-9	...	...	...	...	...	...	...	...
CHXR 57	24835	Cam1 115	...	...	...	...	...	CHXR 57	...	...	E4-4	...	...	...	...	...	B52	...	...
Hn 18	25026	Cam1 116	...	...	...	...	...	...	...	Hn 18	...	...	...	...	...	...	...	...	...
CHXR 59	25148	Cam1 117	...	...	...	...	...	CHXR 59	...	...	E1-4	...	...	...	...	...	...	...	...
CHXR 60	25253	Cam1 118	...	...	...	...	...	CHXR 60	...	Hn 19	...	...	...	...	...	...	...	...	...
IRAS 11120−7750	25283	...	...	...	...	...	...	...	...	...	...	...	...	...	...	...	...	11120−7750	...
T55	25420	Cam1 119	...	T55	Sz 44	...	...	CHXR 61	...	...	E1-6	...	...	...	...	...	...	...	...
CHXR 62	27295	Cam1 120	...	...	...	...	...	CHXR 62	...	Hn 20	...	...	...	...	...	...	...	...	...
Hn 21W	27714	Cam1 121	...	...	...	...	...	...	...	Hn 21W	...	...	...	...	...	...	...	...	...
Hn 21E	27789	Cam1 122	...	...	...	...	...	...	...	Hn 21E	...	...	...	...	...	...	...	...	...
B53	28885	Cam1 123	...	...	...	...	...	...	...	...	...	...	...	...	...	...	B53	...	...
CHXR 65B	32606	...	...	...	...	...	...	CHXR 65B	...	...	...	...	...	...	...	...	...	...	...
CHXR 65A	32644	Cam1 124	...	...	...	...	...	CHXR 65A	...	...	...	...	...	...	...	...	B54	...	...
T56	...	Cam1 125	...	T56	Sz 45	...	HM 32	CHXR 66	...	...	...	HBC 590	...	...	...	...	...	11159−7648	...
CHXR 68B	...	...	...	...	...	...	...	CHXR 68B	...	...	...	...	...	...	...	...	...	...	...
CHXR 68A	...	Cam1 126	...	...	...	...	...	CHXR 68A	...	...	...	...	...	...	...	...	...	...	...
IRAS 11248−7653	...	...	...	...	...	...	...	...	...	...	...	...	...	...	...	...	...	11248−7653	...

NOTES.—(CHSM) Identification number from this study; (CAM98) Cam1 from Table 1 and Cam2 from Table 2 in Cambrésy et al. 1998; (GCVS) General Catalog of Variable Stars, see López & Girard 1990; (W87) Whittet et al. 1987; (Sz77) Schwartz 1977; (Hoff63) Hoffmeister 1963; (HM73) Henize & Mendoza 1973; (F93) Feigelson et al. 1993; (FK89) Feigelson & Kriss 1989; (Hn93) Hartigan 1993; (H82/J85) Hyland et al. 1982 and Jones et al. 1985; (HBC88) Herbig Bell Catalog; (P00) Persi et al. 2000; (KG01) Kenyon & Gómez 2001; (GK01) Gómez & Kenyon 2001; (OTS99) Oasa et al. 1999; (B94) Baud et al. 1984.

REFERENCES

Alcalá, J. M., Krautter, J., Schmitt, J. H. M. M., Covino, E., Wichmann, R., & Mundt, R. 1995, A&AS, 114, 109
Appenzeller, I. 1977, A&A, 61, 21
———. 1979, A&A, 71, 305
Appenzeller, I., Jankovics, I., & Krautter, J. 1983, A&AS, 53, 291
Assendorp, R., Wesselius, P. R., Whittet, D. C. B., & Prusti, T. 1990, MNRAS, 247, 624
Baud, B., et al. 1984, ApJ, 278, L53
Bessell, M. S., & Brett, J. M. 1988, PASP, 100, 1134
Cambrésy, L., Copet, E., Epchtein, N., de Batz, B., Borsenberger, J., Fouqué, P., Kimeswenger, S., & Tiphène, D. 1998, A&A, 338, 977
Carpenter, J. M. 2001, AJ, 121, 2851
Carpenter, J. M., Hillenbrand, L. A., & Skrutskie, M. F. 2001, AJ, 121, 3160 (CHS01)
Cohen, J. G., Grogel, J. A., Perrson, S. E., & Elias, J. H. 1981, ApJ, 249, 481
Comerón, F., Neuhäuser, R., & Kaas, A. A. 2000, A&A, 359, 269
Comerón, F., Rieke, G. H., & Neuhäuser, R. 1999, A&A, 343, 477
Cutri, R. M., et al. 2000, Explanatory Supplement to the 2MASS Second Incremental Data Release (Pasadena: IPAC)
D'Antona, F., & Mazzitelli, I. 1997, Mem. Soc. Astron. Italiana, 68, 807
———. 1998, in ASP Conf. Ser. 134, Brown Dwarfs and Extrasolar Planets, ed. R. Rebolo, E. L. Martin, & M. R. Zapatero-Osorio (San Francisco: ASP), 442
Feigelson, E. D., Casanova, S., Montmerle, T., & Guibert, J. 1993, ApJ, 416, 623
Feigelson, E. D., & Kriss, G. A. 1989, ApJ, 338, 262
Gauvin, L. S., & Strom, K. M. 1992, ApJ, 385, 217
Gómez, M., & Kenyon, S. J. 2001, AJ, 121, 974
Gómez, M., & Persi, P. 2002, A&A, in press
Hartigan, P. 1993, AJ, 105, 1511
Henize, K. G., & Mendoza, E. E. 1973, ApJ, 180, 115
Hoffmeister, C. 1962, Z. Astrophys., 55, 290
———. 1963, Veröff. Sternw. Sonneberg, 6, 1
Huenemoerder, D. P., Lawson, W. A., & Feigelson, E. D. 1994, MNRAS, 271, 967
Hyland, A. R., Jones, T. J., & Mitchell, R. M. 1982, MNRAS, 201, 1095
Jones, T. J., Hyland, A. R., Harvey, P. M., Wilking, B. A., & Joy, M. 1985, AJ, 90, 1191
Kenyon, S. J., & Gómez, M. 2001, AJ, 121, 2673
Kirkpatrick, J. D., et al. 1999, ApJ, 519, 802
Kirkpatrick, J. D., et al. 2000, AJ, 120, 447
Lada, C. J., & Adams, F. C. 1992, ApJ, 393, 278
Lawson, W. A., Feigelson, E. D., & Huenemoerder, D. P. 1996, MNRAS, 280, 1071
Leggett, S. K., et al. 2002, ApJ, 564, 452
Lehtinen, K., Haikala, L. K., Mattila, K., & Lemke, D. 2001, A&A, 367, 311
López, C. E., & Girard, T. M. 1990, PASP, 102, 1018
Luhman, K. L., Rieke, G. H., Young, E. T., Cotera, A. S., Chen, H., Rieke, M. J., Schneider, G., & Thompson, R. I. 2000, ApJ, 540, 1016
Mamajek, E. E., & Feigelson, E. D. 2001, in ASP Conf. Ser. 244, Young Stars Near Earth: Progress and Prospects, ed. R. Jayawardhana & T. Greene (San Francisco: ASP), 104
Mannucci, F., Basile, F., Poggianti, B., Cimatti, A., Daddi, E., Pozzetti, L., & Vanzi, L. 2001, MNRAS, 326, 745
Meyer, M. R., Calvet, N., & Hillenbrand, L. A. 1997, AJ, 114, 288
Nordh, L., et al. 1996, A&A, 315, L185
Oasa, Y., Tamaura, M., & Sugitani, K. 1999, ApJ, 526, 336
Persi, P., et al. 2000, A&A, 357, 219
Prusti, T., Clark, F. O., Whittet, D. C. B., Laureijs, R. J., & Zhang, C. Y. 1991, MNRAS, 251, 303
Rydgren, A. E. 1980, AJ, 85, 444
Schwartz, R. D. 1977, ApJS, 35, 161
———. 1991, in Low-Mass Star Formation in Southern Molecular Clouds, ed. B. Reipurth (Garching: ESO), 93
Skrutskie, M. F., Meyer, M. R., Whalen, D., & Hamilton, C. 1996, AJ, 112, 2168
Songaila, A., Cowie, L. L., Hu, E. M., & Gardner, J. P. 1994, ApJS, 94, 461
Stetson, P. B. 1996, PASP, 108, 851
Väisänen, P., Tollestrup, E. V., Willner, S. P., & Cohen, M. 2000, ApJ, 540, 593
Wainscoat, R. J., Cohen, M., Volk, K., Walker, H. J., & Schwartz, D. E. 1992, ApJS, 83, 111
Walter, F. M. 1992, AJ, 104, 758
Whittet, D. C. B., Kirrane, T. M., Kilkenny, D., Oates, A. P., Watson, F. G., & King, D. J. 1987, MNRAS, 224, 497
Whittet, D. C. B., Prusti, T., Franco, G. A. P., Gerakines, P. A., Kilkenny, D., Larson, K. A., & Wesselius, P. R. 1997, A&A, 327, 1194
Whittet, D. C. B., Prusti, T., & Wesselius, P. R. 1991, MNRAS, 249, 319
Winterberg, J., & Bruch, A. 1996, Inf. Bull. Variable Stars, No. 4334